Monoubiquitination of Histone H2B Blocks Eviction of Histone Variant H2A.Z from Inducible Enhancers

Segala, Grégory; Bennesch, Marcela; Pandey, Deo Prakash; Hulo, Nicolas; Picard, Didier

How to cite

SEGALA, Grégory et al. Monoubiquitination of Histone H2B Blocks Eviction of Histone Variant H2A.Z from Inducible Enhancers. In: Molecular cell, 2016, vol. 64, n° 2, p. 334–346. doi: 10.1016/j.molcel.2016.08.034

This publication URL: https://archive-ouverte.unige.ch/unige:88395
Publication DOI: 10.1016/j.molcel.2016.08.034

Monoubiquitination of histone H2B blocks eviction of histone variant H2A.Z from inducible enhancers

Gregory Segala[1,2], Marcela A. Bennesch[1,2], Deo Prakash Pandey[1,3], Nicolas Hulo[2] and Didier Picard[1,2]*

[1] Département de Biologie Cellulaire

and [2] Institute of Genetics and Genomics of Geneva

Université de Genève

CH-1211 Genève 4, Switzerland

[3] Present adress: Biotech Research and Innovation Center (BRIC)

University of Copenhagen

2200 Copenhagen, Denmark

* corresponding author

Phone: +41 22 379 6813

Email: didier.picard@unige.ch

SUMMARY

Covalent modifications of histones play a crucial role in the regulation of gene expression. Histone H2B monoubiquitination has mainly been described as a regulator of transcription elongation, but its role in transcription initiation is poorly documented. We investigated the role of this histone mark (H2Bub1) on different inducible enhancers, in particular those regulated by the estrogen receptor α, by loss and gain of function experiments with the specific E3-ubiquitin ligase complex of H2B: RNF20/RNF40. RNF20/RNF40 overexpression causes repression of the induced activity of these enhancers. Genome-wide profiles show that H2Bub1 levels are negatively correlated with the accessibility of enhancers to transcriptional activators. We found that the chromatin association of histone variant H2A.Z, which is evicted from enhancers for transcriptional activation, is stabilized by H2Bub1 by impairing access of the chromatin remodeler INO80. We propose that H2Bub1 acts as a gatekeeper of H2A.Z eviction and activation of inducible enhancers.

INTRODUCTION

In eukaryotes, gene expression is challenged by the fact that DNA is wrapped around nucleosomes, which imposes a physical constraint for the access of transcription factors and RNA polymerases to DNA (Teves et al., 2014). Some regulatory regions of the genome, including enhancers, insulators and promoters, need to be partly accessible to transacting factors to allow the regulation and adaptation of gene expression. Post-translational modifications of histones and the replacement of histones by histone variants have emerged as the central mechanisms by which cells regulate the stability of the nucleosomes at defined regions of the genome (Venkatesh and Workman, 2015). Post-translational modifications of histones can have activator or repressive roles for gene expression by affecting chromatin accessibility (Zentner and Henikoff, 2013).

H2B monoubiquitination (H2Bub1) is a conserved histone mark present in fungi, plants and mammals (Weake and Workman, 2008) indicating an essential role in eukaryotes. In mammals, the heterodimeric proteins RNF20/RNF40 are the specific E3-ubiquitin ligases for H2B (Zhu et al., 2005). H2Bub1 was found to decrease strongly in primary tumor samples of late stage breast cancer, suggesting a tumor suppressor role of H2Bub1 (Prenzel et al., 2011). In line with this hypothesis, estrogen-dependent breast cancer cells are able to proliferate without estrogen when RNF40 is knocked down (Prenzel et al., 2011). Surprisingly, the inactivation of RNF20/40 only has a moderate effect on overall gene expression levels (Shema et al., 2008), raising the possibility that the H2Bub1 chromatin mark could be dedicated to the regulation of specific groups of genes rather than the regulation of the whole

genome. Indeed, H2Bub1 has been associated with the regulation of inducible genes involved in cell differentiation (Zhu et al., 2005; Fuchs et al., 2012; Karpiuk et al., 2012; Materne et al., 2016) and inflammation (Tarcic et al., 2016), suggesting a role for H2Bub1 in the regulation of inducible rather than constitutive transcription. Genomic analyses showed that H2Bub1 is enriched in actively transcribed regions of human genes (Minsky et al., 2008) and it has been proposed to be involved in the regulation of global transcriptional elongation (Pavri et al., 2006; Minsky et al., 2008). In support of this notion, it was shown that H2B monoubiquitination regulates nucleosome reassembly during transcriptional elongation (Fleming et al., 2008) and that the cotranscriptional monoubiquitination of H2B is tightly coupled with the elongation rate of RNA polymerase II (Fuchs et al., 2014). Interestingly, it has been pointed out that H2Bub1 could be an activator in transcribed regions while having a repressive function in promoters (Batta et al., 2011; Materne et al., 2016), but the underlying molecular mechanisms have not been studied. These preliminary observations raise the possibility that H2Bub1 could be involved in regulating transcription initiation, which might explain why H2Bub1 depletion could have gene-specific effects. This speculation is further supported by the fact that the H2B deubiquitinase USP22 is part of the coactivator complex SAGA and is required for the activation of transcription (Zhang et al., 2008).

Transcription initiation is strongly regulated by genetic elements called enhancers. Enhancers contain DNA motifs that are recognized by specific transcription factors. These transcription factors, their coregulators and the chromatin organization determine when and where these enhancers will be active to stimulate the transcription of their target genes (Shlyueva et al., 2014). The composition of the

chromatin of regulatory elements is enriched by specific histone marks and some histone variants. Several histone marks like H3K27ac or H3K27me3, which regulate positively or negatively gene expression, respectively, define the activity of enhancers (Shlyueva et al., 2014). The histone variants H2A.Z and H3.3 are incorporated at the level of regulatory elements such as enhancers and promoters. Nucleosomes containing these two variants are particularly unstable (Jin et al., 2009), which makes these chromatin regions dynamic and more easily accessible to transacting factors. The histone variant H2A.Z was described as an essential determinant of the inducible transcriptional activation mediated by the estrogen receptor α (ERα) (Gevry et al., 2009; Brunelle et al., 2015). Despite its positive role for gene activation, it was found that H2A.Z dissociates from enhancers during inducible gene activation (Gevry et al., 2009; Chauhan and Boyd, 2012), maybe in the course of nucleosome disassembly (Papamichos-Chronakis et al., 2011; Yen et al., 2013). Importantly, there could be a crosstalk between histone modifications and H2A.Z dynamics as it was reported that the H2A.Z distribution across the genome can be controlled by H3K56ac, since this alters the deposition of H2A.Z by the SWR-C remodeling enzyme (Watanabe et al., 2013).

Despite considerable progress in the last few decades, the chromatin features at inducible enhancers that allow and promote rapid and reversible activation are still incompletely understood. Considering the possibility that H2Bub1 could be involved in regulating transcription initiation, we decided to explore the hypothesis that H2Bub1 regulates inducible rather than constitutive enhancers by using the transcriptional regulation by nuclear receptors such as ERα as a model system. These ligand-activatable transcription factors rapidly trigger the activation of specific

inducible enhancers in response to their cognate ligand. This affords the unique opportunity to explore chromatin determinants of inducible enhancers very easily before and after activation.

RESULTS

RNF20/40 repress inducible enhancers

We performed experiments with a panel of luciferase reporter gene constructs controlled by the estrogen receptor α (ERα, induced by 17β-estradiol (E2)), the progesterone receptor (PR, induced by progesterone (P4)) or the glucocorticoid receptor (GR, induced by Dexamethasone (Dex)) transfected into human HEK293T cells (Figure 1A to 1D). Overexpression of RNF20 or RNF40 and especially their concomitant overexpression inhibited the induction of these enhancers without significant effects on their basal levels. This inhibitory effect depends on the presence of an inducible enhancer because a construct devoid of any enhancer is not sensitive to the effect of RNF20/40 (Figure 1E). Conversely, we confirmed that RNF20/40 repress enhancer activity by knockdown experiments with two different shRNAs each (Figures 1F and S1A to S1G). This repressive effect is independent of cell context as it could also be observed with breast and lung cancer cells (Figures 1G, S1H and S1I). The levels of the corresponding transcription factor, ERα, were not affected by RNF20/40 knockdown or overexpression whereas corresponding changes could be seen for the H2Bub1 levels (Figures 1H and S1J). Our results mirrored the fact that RNF20/40 function as a heterodimer (Zhu et al., 2005; Pavri et al., 2006), since the combined overexpression was more efficient (Figure S1J) and

the knockdown of either one, as previously reported (Pavri et al., 2006), was as efficient as their combined knockdown (Figure 1H). To corroborate further that RNF20/40 specifically act on inducible enhancers, we used chimeras consisting of the Gal4 DNA binding domain fused to either the N-terminal or the ligand binding domains of ERα, which are responsible for its constitutive or inducible transactivation activities, respectively (Bennesch and Picard, 2015). Only the inducible chimeric transcription factor proved to be affected by RNF20/40 (Figures 1I and 1J). The overexpression of H2B by itself repressed the enhancer activity and impaired the repression by RNF20/40, perhaps by flooding cells with an excess of H2B. In comparison to wild-type H2B, the overexpression of the H2B monoubiquitination mutant K120R recapitulated the de-repressive effect of the knockdown of RNF20/40 (Figure 1K). Parallel experiments with the proteasome inhibitor MG132 supported the conclusion that RNF20/40 repress inducible enhancers through the monoubiquitination of H2B independently of proteasomal degradation (Figure S1K).

RNF20/40 inhibit endogenous ERα target gene expression by repressing inducible enhancers

We then examined the role of RNF20/40 for the regulation of endogenous ERα target genes in MDA-MB134 breast cancer cells, which we have used interchangeably with MCF-7 cells. The knockdown of RNF20/40 stimulated the E2-induced expression of a panel of ERα target genes (Figures 2A to 2F). To assess more directly the activity of the enhancers that regulate the expression of the two ERα target genes *GREB1* and *TFF1*, we measured the production of the associated enhancer RNAs (eRNA), which are transcribed in both orientations (Li et al., 2013). The activities of the enhancers of *GREB1* and *TFF1* are stimulated by the knockdown of RNF20/40, and this correlates

with an increase of the recruitment of ERα and the pioneer factor FOXA1 (Hurtado et al., 2011) to these enhancers (Figures 2G to 2L, S2B and S2C), without any change of the total FOXA1 protein levels (Figure S2A). These results suggest that RNF20/40 repress inducible enhancers by decreasing the recruitment of key transcription factors, possibly as a result of shaping the chromatin environnment around these enhancers.

H2Bub1 is depleted from the core of inducible enhancers and open chromatin

We therefore explored the genome-wide chromatin immunoprecipitation (ChIP-seq) profiles of H2Bub1, ERα, the coactivators Med1 and P300 and the chromatin accessibility (DNase-seq) using publicly available datasets (He et al., 2012; Liu et al., 2014; Nagarajan et al., 2014) for MCF7 breast cancer cells (Figure 3A). As expected, H2Bub1 is increased across the ERα target genes *GREB1* and *TFF1* upon induction by E2. However, at the level of the inducible enhancers, characterized by the colocalization of ERα, Med1, P300 and DNase hypersensitive sites (DHS), the relative levels of H2Bub1 display a drastic drop. We then grouped the ERα binding sites (ERBS) according to their strength and observed that the H2Bub1 signal across the ERBS is proportional to the strength of the ERBS. Interestingly, there is a relative drop of H2Bub1 levels, hereafter referred to as an “H2Bub1 valley”, at the center of high ERBS independently of any induction (Figure 3B to 3D). To ascertain that these valleys genuinely exist relative to total H2B bound at these sites, we had to resort to a higher resolution method. We closely examined the relative levels of H2Bub1 over H2B at the *GREB1* and *TFF1* enhancers at nucleosomal resolution by digesting chromatin with micrococcal nuclease (MNase) for ChIP assays. Again, H2Bub1 valleys could clearly be seen at the centers of these enhancers, even upon

standardizing to total H2B (Figure S3A). Induction by E2 further accentuates H2Bub1 valleys in a statistically significant fashion at the center of high ERBS while a peak of H2Bub1 is observed for low ERBS and the combination of all types of ERBS (Figures 3C to 3D, and S3B). A kinetic analysis by ChIP of the H2Bub1/H2B ratio at the centers of the *GREB1* and *TFF1* enhancers showed that H2Bub1 levels drop strongly by 30 minutes following induction by E2 and that low levels are maintained thereafter (Figure 3E), further supporting the genome-wide data.

Importantly, pronounced H2Bub1 valleys coincide with several other hallmarks of active enhancers and regulatory sequences including Med1 and P300 binding, DHS, and transcription start sites (TSS) (Figures 3F to 3H, and S3C). This implied that H2Bub1 valleys are more generally associated with active enhancers and chromatin regions that need to be accessible to regulatory factors. To clarify this issue, we called the broad peaks of H2Bub1 and bioinformatically extracted the gaps between the peaks as valleys (Figure S3D and S3E). We observed roughly opposite profiles of chromatin accessibility and nucleosome occupancy for H2Bub1 peaks and H2Bub1 valleys, which suggested an involvement of H2Bub1 in nucleosome stabilization (Figure 3I and 3J), as previously proposed (Chandrasekharan et al., 2009). Repressive histone marks like H3K9me3 and H3K27me3 are decreased in H2Bub1 valleys but increased in H2Bub1 peaks, while it is exactly the opposite for the active enhancer mark H3K27ac (Figure S3F to S3I). Even if the induction by E2 modifies the intensity of the signals, the profiles are independent of any induction, consistent with the idea that the chromatin environment is already preset before induction. H2Bub1 levels seem to be specific to enhancer-related histone marks since no clear profile was observed for the insulator factor CTCF (Figure S3J). These

results demonstrated that regions comprising highly active inducible enhancers are characterized by high levels of H2Bub1 that drop at the level of the transcriptional activator binding sites, presumably to increase chromatin accessibility to these factors.

H2Bub1 stabilizes the association of H2A.Z with inducible enhancers

In the nucleosome, H2B forms dimers with H2A or H2A variants, of which H2A.Z is preferentially found at TSS and enhancers (Jin et al., 2009; Dalvai et al., 2013; Brunelle et al., 2015). In agreement with this, we found that H2A.Z levels increase with the strength of the ERBS, independently of any induction (Figures 4A and S4A). Interestingly, H2Bub1 forms valleys on H2A.Z binding sites and the average signal of H2Bub1 positively correlates with the average signal of H2A.Z across strong ERBS (Figure 4B and 4C). This suggests that H2Bub1 could be involved in the stabilization of H2A.Z in nucleosomes. In turn, an H2Bub1 valley at the center of H2A.Z binding sites could favor a destabilization of H2A.Z and promote chromatin accessibility. A time-course experiment by ChIP of H2A.Z on the *GREB1* and *TFF1* enhancers confirmed that the levels of chromatin-associated H2A.Z decrease upon E2 induction while the binding of ERα concomitantly increases (Figure 4D). Most importantly, upon impairing H2B monoubiquitination, H2A.Z strongly decreases on the *GREB1* and *TFF1* enhancers before and after E2 induction (Figure 4E and 4F). We concluded from these results that H2Bub1 specifically stabilizes H2A.Z on inducible enhancers since no striking effects were observed for H2A.Z on TSS and for H2B itself (Figure S4B to S4G). For H2B, which would get evicted from enhancers along with H2A.Z, it must be mentioned that it could be reincorporated into nucleosomes with H2A (Papamichos-Chronakis et al., 2011).

To generate more direct evidence that it is indeed H2B monoubiquitination that stabilizes H2A.Z, we used the H2B monoubiquitination mutant K120R. Upon overexpressing the mutant compared to wild-type H2B, we observed a decrease of H2A.Z on the *GREB1* and *TFF1* enhancers (Figure 4G). As we had shown that H2B monoubiquitination also regulates transfected reporter gene constructs (Figure 1B to 1D), we wanted to provide further support for the stabilizing effect of H2Bub1 on H2A.Z with this system. An H2A.Z ChIP experiment with an ERα-dependent enhancer of a luciferase reporter showed that overexpression of RNF20 and RNF40 increases the stability of H2A.Z both without and with induction by E2 (Figure 4H). Lending further support to the validity of using transfected reporter plasmids, we confirmed with this construct that the induction by E2 decreases H2A.Z levels on the enhancer. The effect of H2B monoubiquitination on H2A.Z dynamics is general enough to be seen by co-immunoprecipitation as the overexpression of RNF20 and RNF40 increases the association of H2B with H2A.Z (Figure 4I). This suggests that H2B monoubiquitination affects the dynamics of association/dissociation of H2B with H2A.Z. H2Bub1 and H2A.Z have been linked to the transcription of antisense RNA (Zofall et al., 2009; Murray et al., 2015), which could arise from cryptic transcription initiation in gene bodies (Smolle and Workman, 2013). Indeed, impairing H2B monoubiquitination increases the production of antisense RNA in the *GREB1* and *TFF1* gene bodies (Figure 4J and 4K), indicating that H2Bub1 could play a role in controlling the H2A.Z dynamics to avoid unspecific transcription initiation.

H2Bub1 impairs the interaction of INO80 with inducible enhancers

H2Bub1 could stabilize H2A.Z either by promoting its incorporation into nucleosomes or by blocking its eviction (Gerhold and Gasser, 2014). To gain insights into the

proteins that could link H2A.Z dynamics with H2Bub1, we generated an *in silico* interactome of RNF20/40 based on data from public repositories (Figure 5A). This revealed an interaction between RNF40 and the chromatin remodeler INO80, already known to be involved in the eviction of H2A.Z (Papamichos-Chronakis et al., 2011), and ERα, as previously hinted at (Bedi et al., 2015). We first assessed whether the protein levels of INO80 are affected by the RNF20/40 knockdown; while H2Bub1 levels decreased, INO80 levels remained unchanged both in MDA-MB134 and in HEK293T cells (Figure 5B). We then experimentally confirmed by several reciprocal co-immunoprecipitation experiments that INO80 interacts with RNF40 (Figure 5C), and that RNF40 interacts with ERα as well as RNA polymerase II (Figure S5A and S5B). Considering that RNF40 and RNF20 form a heterodimer, it was unexpected that we failed to co-immunoprecipitate RNF20 with INO80, ERα and RNA polymerase II. At this point, we can only speculate that interactions of RNF20 with other proteins may be more labile or that the epitopes, on which we relied, are masked or that the antibodies used interfered with these particular RNF20 complexes. We cannot formally exclude that the INO80-RNF40 complex is devoid of RNF20, but clarifying the functional relevance of this interaction and of the unusual prospect of RNF40 acting independently of RNF20 will require further investigation.

INO80 appears to interact more strongly with ERα upon induction by E2 (Figure 5C). This suggested that INO80 could be part of transactivator complexes. The knockdown of INO80 reduced the stimulation of the endogenous *GREB1* and *TFF1* enhancers by RNF20/40 silencing (Figure 5D). Moreover, similar results were obtained with a transfected reporter gene assay: the knockdown of INO80 but not

that of the H2A.Z chaperone ANP32E (Obri et al., 2014) significantly reduced the stimulation of the E2-inducible enhancer by RNF20/40 silencing (Figures 5E and S5C). We also noticed that the knockdown of INO80 by itself, but not that of ANP32E, decreased the activity of the E2-inducible enhancer (Figure 5F). Consistent with the proposed antagonistic relationship between H2Bub1 and INO80 recruitment, the recruitment of INO80 is increased on the *GREB1* and *TFF1* enhancers upon E2 induction and further boosted by the knockdown of RNF40 (Figure 5G). To ascertain that these effects are indeed due to changes in H2Bub1 levels, we demonstrated that the levels of INO80 on the *GREB1* and *TFF1* enhancers are increased upon overexpression of the monoubiquitination mutant of H2B (Figure 5H). Conversely, the stimulation of H2B monoubiquitination by RNF20/40 overexpression decreases the recruitment of INO80 to an ERα-dependent enhancer, here in the context of a transfected reporter plasmid (Figure 5I). Finally, co-immunoprecipitation experiments demonstrated that overexpression of RNF20/40 decreases the interaction of INO80 with wild-type H2B (Figure 5J). Moreover, the interaction between INO80 and the monoubiquitination mutant of H2B is stronger than with wild-type H2B and insensitive to the overexpression of RNF20/40 (Figure 5J). Thus, H2Bub1 represses inducible enhancers by interfering with the recruitment of INO80 and the resulting eviction of H2A.Z.

DISCUSSION

We have discovered a repressive role for the monoubiquitination of H2B for inducible transcription and suggested a molecular mechanism based on our study. In our

model (Figure 6) the chromatin at inducible enhancers could be primed by the distribution and relative abundance of H2A.Z and H2Bub1 before induction. We have discovered that both H2A.Z and H2Bub1 are enriched at regulatory sequences of induced genes (Figures 3B, 4A and S4A) with a notable relative decrease of H2Bub1 at the very center of strong inducible enhancers, a feature we have referred to as an H2Bub1 valley (Figure 3B, 3D and S3A). We hypothesize that the eviction of the H2A.Z/H2B dimer by INO80 is impaired by H2Bub1, and therefore, that the reduced levels of H2Bub1 at the center of inducible enhancers direct the eviction of H2A.Z/H2B to this location to maintain a defined region accessible to transcription factors and their coactivators such as Med1 and P300. Upon induction, the levels of H2Bub1 decrease further at the center of inducible enhancers while they increase on both sides surrounding these enhancers (Figure 3D). An H2Bub1 deubiquitinase (DUB) such as USP22, which is associated with the coactivator complex SAGA (Zhang et al., 2008) or the proteasome-associated DUB Uch37, which can be recruited by INO80 itself (Yao et al., 2008), could be responsible for removing the H2Bub1 mark from the center of the induced enhancers. Because of the stabilization of H2A.Z-containing nucleosomes by H2Bub1 through the stabilization of H2A.Z/H2B dimers, the increase of H2Bub1 on both sides of the induced enhancer could prevent the spreading of accessible chromatin. Since INO80 interacts with active transcription factor complexes (Cai et al., 2007, and Figure 5C), it is conceivable that it also removes H2A.Z/H2B dimers in the immediate vicinity to favor the recruitment of additional transcription factors. Moreover, this process could be facilitated by the INO80-associated DUB Uch37. This could contribute to forming the complex transcription factor hubs previously characterized for nuclear receptors and other transcription factors (see for example Liu et al., 2014).

There are several possibilities to explain the stabilization of H2A.Z in the chromatin of strong inducible enhancers by H2Bub1. Like histones, ubiquitin is a lysine-rich protein and therefore, the stabilizing effect of H2Bub1 on the nucleosome could be mediated by an increased affinity for DNA (Chandrasekharan et al., 2009). This could strengthen the contact between the H2B-H2A.Z dimer and DNA and increase the energy barrier for its eviction by the ATP-dependent chromatin remodeler INO80. An alternative but not mutually exclusive explanation rests on our finding that H2Bub1 inhibits the binding of INO80 to strong inducible enhancers (Figure 5G). It is conceivable that the coupling of an ubiquitin molecule to H2B could impair the interaction of INO80 with the nucleosome because of steric hindrance. Indeed, the conjugation of an ubiquitin molecule to H2B is a very bulky modification of the core of the protein that represents half of its mass. This second explanation is supported by our finding that the interaction of INO80 with H2B is decreased by the monoubiquitination of H2B (Figure 5J), and by the detailed interaction map of the nucleosome with the INO80 complex, recently determined by mass spectrometry (Tosi et al., 2013). Some interactions between H2B of *Drosophila melanogaster* and several components of the INO80 complex were mapped to K118, the H2B ubiquitination site in this organism. The juxtaposition of the conjugated ubiquitin with the interaction site could prevent the binding of essential components of the INO80 complex to the nucleosome, and thereby, the INO80-mediated eviction of H2B/H2A.Z dimers. Ultimately, reconstitution experiments with chemically ubiquitylated H2B and other purified components (Zhou et al., 2016) could help to dissect the molecular details of this remodeling reaction.

One of the findings that appears confusing at first sight relates to the global distribution of H2Bub1 on inducible enhancers. We found that H2Bub1 and H2A.Z levels are positively correlated on strong inducible enhancers (Figure 4C) and that their respective abundances increase proportionally with the strength of the inducible enhancers (Figures 3B, 4A and S4A). This suggests that proteins responsible for the H2Bub1 mark could somehow be functionally linked to the proteins involved in H2A.Z dynamics. Indeed, we found that INO80 interacts with RNF40 (Figure 5C), but there could be additional interactions between other players of the H2Bub1 and H2A.Z pathways. Identifying these interactions and determining their functional consequences could help to explain the functional relationship that may link the distribution of H2Bub1 with H2A.Z and more generally with the strength of the inducible enhancers.

By analogy to the increase in H2Bub1 levels within the gene bodies that arises from transcriptional elongation by RNA polymerase II (Minsky et al., 2008; Fuchs et al., 2014), we hypothesize that the transcription of eRNAs on both sides of the enhancer could explain the observed increase of H2Bub1 levels. In contrast, the observed decrease of H2Bub1 levels at the center of activated inducible enhancers could be due to deubiquitination by the SAGA complex. This speculation is supported by the characterization of USP22, the deubiquitinase subunit of SAGA, as a coactivator of the androgen receptor, another member of the superfamily of nuclear receptors (Zhao et al., 2008). Since H2Bub1 valleys are found exactly where transcriptional activators bind (Figures 3F and 3G), this suggests that upon induction H2Bub1 is further deubiquitinated where H2A.Z has to be evicted by INO80 to allow additional transcriptional activators to gain access to the DNA. However, since there are

already H2Bub1 valleys at the center of inducible enhancers before induction, albeit less pronounced than after induction, this suggests that additional mechanisms are involved in setting up the initial H2Bub1 distribution.

We demonstrated that INO80 interacts with ERα (Figure 5C) and presumably other transcriptional activators and that it is preferentially recruited to activated inducible enhancers (Figure 5G). Consistent with our results showing a time-dependent reduction of H2A.Z at inducible enhancers after activation (Figure 4D), this suggests that the eviction of H2A.Z by INO80 is necessary for inducible enhancer activation by the recruitment of transcriptional activators. This is in agreement with several studies that had highlighted a role of INO80 as transcriptional coactivator (Cai et al., 2007; Li et al., 2012; Wang et al., 2014). Thus, this complements the role of INO80 in promoting the turnover of H2A.Z-containing nucleosomes (Yen et al., 2013) and its contribution to their disassembly following gene activation (Papamichos-Chronakis et al., 2011; Yen et al., 2013).

The genomic distribution of H2A.Z has been demonstrated to be controlled by FACT to avoid its misincorporation into chromatin, which would contribute to the formation of cryptic initiation sites (Jeronimo et al., 2015). In turn, we showed that the reduction of H2Bub1 leads to an increase of cryptic transcripts during target gene activation (Figure 4J and 4K). These results suggest that a tight spatial control of the distribution of H2A.Z may be exerted by FACT and H2Bub1 to avoid the generation of cryptic sites and to prevent transcription initiation at these sites, respectively. Moreover, as H2Bub1 and FACT were described to function cooperatively in

transcriptional elongation (Pavri et al., 2006), they may also control the distribution and dynamics of H2A.Z in a cooperative manner.

While H2Bub1 has been considered to be primarily a regulator of transcriptional elongation, we have demonstrated that H2Bub1 plays an essential role for the regulation of inducible enhancers by acting as a gatekeeper of H2A.Z eviction. In the future, the interplay between H2Bub1 and H2A.Z should be studied in more detail to determine how general it is for inducible enhancers and whether it is restricted to inducible enhancers or at play at other regulatory elements in the genome as well. The mechanism that we have highlighted should also prompt studies on the activator role of H2B deubiquitinases for transcription initiation and on additional aspects of the architecture of inducible enhancers and their regulation.

EXPERIMENTAL PROCEDURES

See Supplemental experimental procedures for additional details.

Cell culture

Induction of ERα was done with 100 nM 17β-estradiol (Sigma-Aldrich), of GR with 100 nM dexamethasone (Sigma-Aldrich) and of PR with 100 nM progesterone (Sigma-Aldrich). Transfections were performed with the Polyethylenimine (PEI) transfection reagent mixed with DNA at a DNA:PEI ratio of 1:3. Knockdowns were generated by infection with lentiviruses expressing specific shRNA against each targeted mRNA.

Luciferase assays

Cells were lysed using the Passive Lysis Buffer (Promega) and firefly luciferase and Renilla activities were measured in cell lysates with the Dual-Luciferase kit (Promega) with a bioluminescence plate reader. Renilla activity was used as a transfection control.

Reverse-transcription and quantitative PCR

For the quantification of antisense RNA, specific primers instead of random primers were used for the reverse-transcription (Supplementary Table S1). In qPCR experiments, RNA levels were standardized with *GAPDH* as the internal standard.

Chromatin immunoprecipitation (ChIP)

The protocol for ChIP experiments is the one described by Schmidt *et al*. (Schmidt et al., 2009). ChIP values were standardized with internal controls (the *c-MYC* intron for the ChIP of ERα and FOXA1, or the *GAPDH* coding region for the ChIP of H2A.Z, H4, H2Bub1, H2B and INO80) and normalized with the input values.

ChIP-seq data re-analyses and interactome

The following ChIP-seq datasets, available publicly on the NCBI server, were used: GSE55921 (H2Bub1 and ERα) (Nagarajan et al., 2014), GSE60270 (Med1, P300) (Liu et al., 2014), GSE33216 (DNase-seq) (He et al., 2012), GSE51097 (MNase-seq) (Shimbo et al., 2013), GSE23701 (H3K9me3 and H3K27me3) (Joseph et al., 2010),

GSE40129 (H3K27ac) (Theodorou et al., 2013), GSE33213 (CTCF; ENCODE) and GSE57436 (H2A.Z) (Brunelle et al., 2015). SRA files from each dataset were downloaded from the NCBI server, converted into fastq files and mapped to the human reference genome hg19 with bwa mem. Visualization of ChIP-seq profiles was performed with the Integrative Genomics Viewer (version 2.3.67). Peak calling was carried out by using the MACS tool from the Galaxy framework. ERBS were separated into three groups (high, medium and low) by using R based on the confidence level ($-10*\log_{10}$ p-value) of the peak center of ERBS. The “high”, "medium" and "low" groups correspond to ERBS with confidence levels of more than 150, 50 to 150 and less than 50, respectively. H2Bub1 valleys were defined as gaps of less than 50 kb between H2Bub1 peaks, and they were extracted with R. Aggregation plots were done with the Cistrome tool (Galaxy instance). The means of the H2A.Z and H2Bub1 signals on high ERBS were determined by mapping the mean coverage of H2A.Z and H2Bub1 on high ERBS gaps with bedtools map. The scatterplot, linear regression, and calculations of the coefficient of determination (r^2) and p-value were done with R. The combined interactome of RNF20 and RNF40 was obtained with the PPiMapBuilder plug-in (https://github.com/PPiMapBuilder/PPiMapBuilder; developed based on a previous study (Echeverria et al., 2011)) of the Cytoscape freeware on all of the available interactome databases and organisms proposed by the plug-in.

Statistical analyses

The bar graphs show averages of several independent experiments with technical replicates and the errors of the means. Statistical significance was determined with the Student’s t test.

SUPPLEMENTAL INFORMATION

Supplemental Information includes five figures, two tables, and Supplemental Experimental Procedures.

AUTHOR CONTRIBUTIONS

GS and DP designed the experiments; GS performed the vast majority of experiments; MAB performed several experiments and DPP made the initial discovery of Bre1/Rad6 in a yeast screen; NH contributed to the bioinformatic analyses; GS, MAB, DPP, NH and DP analysed the data; GS and DP wrote the paper.

ACKNOWLEDGMENTS

We are grateful to Pierre Frey and Kamilla Malinowska for their early efforts in this project, Lilia Bernasconi for technical assistance at the beginning of the project, Julien Soudet and Joan Conaway for helpful discussions, Pierre Dupuis and colleagues for the PPiMapBuilder plug-in, and numerous other colleagues for their gifts of reagents. This work was supported by the Canton de Genève, the Swiss National Science Foundation, and the Fondation Medic.

REFERENCES

Batta, K., Zhang, Z., Yen, K., Goffman, D.B., and Pugh, B.F. (2011). Genome-wide function of H2B ubiquitylation in promoter and genic regions. Genes Dev. *25*, 2254-2265.

Bedi, U., Scheel, A.H., Hennion, M., Begus-Nahrmann, Y., Ruschoff, J., and Johnsen, S.A. (2015). SUPT6H controls estrogen receptor activity and cellular differentiation by multiple epigenomic mechanisms. Oncogene *34*, 465-473.

Bennesch, M.A., and Picard, D. (2015). Minireview: Tipping the balance: ligand-independent activation of steroid receptors. Mol. Endocrinol. *29*, 349-363.

Brunelle, M., Nordell Markovits, A., Rodrigue, S., Lupien, M., Jacques, P.E., and Gevry, N. (2015). The histone variant H2A.Z is an important regulator of enhancer activity. Nucleic Acids Res. *43*, 9742-9756.

Cai, Y., Jin, J., Yao, T., Gottschalk, A.J., Swanson, S.K., Wu, S., Shi, Y., Washburn, M.P., Florens, L., Conaway, R.C. et al. (2007). YY1 functions with INO80 to activate transcription. Nat. Struct. Mol. Biol. *14*, 872-874.

Chandrasekharan, M.B., Huang, F., and Sun, Z.W. (2009). Ubiquitination of histone H2B regulates chromatin dynamics by enhancing nucleosome stability. Proc. Natl. Acad. Sci. USA *106*, 16686-16691.

Chauhan, S., and Boyd, D.D. (2012). Regulation of u-PAR gene expression by H2A.Z is modulated by the MEK-ERK/AP-1 pathway. Nucleic Acids Res. *40*, 600-613.

Dalvai, M., Fleury, L., Bellucci, L., Kocanova, S., and Bystricky, K. (2013). TIP48/Reptin and H2A.Z requirement for initiating chromatin remodeling in estrogen-activated transcription. PLoS Genet. *9*, e1003387.

Echeverria, P.C., Bernthaler, A., Dupuis, P., Mayer, B., and Picard, D. (2011). An interaction network predicted from public data as a discovery tool: application to the Hsp90 molecular chaperone machine. PLoS ONE *6*, e26044.

Fleming, A.B., Kao, C.F., Hillyer, C., Pikaart, M., and Osley, M.A. (2008). H2B ubiquitylation plays a role in nucleosome dynamics during transcription elongation. Mol. Cell *31*, 57-66.

Fuchs, G., Hollander, D., Voichek, Y., Ast, G., and Oren, M. (2014). Cotranscriptional histone H2B monoubiquitylation is tightly coupled with RNA polymerase II elongation rate. Genome Res. *24*, 1572-1583.

Fuchs, G., Shema, E., Vesterman, R., Kotler, E., Wolchinsky, Z., Wilder, S., Golomb, L., Pribluda, A., Zhang, F., Haj-Yahya, M. et al. (2012). RNF20 and USP44 regulate stem cell differentiation by modulating H2B monoubiquitylation. Mol. Cell *46*, 662-673.

Gerhold, C.B., and Gasser, S.M. (2014). INO80 and SWR complexes: relating structure to function in chromatin remodeling. Trends Cell Biol. *24*, 619-631.

Gevry, N., Hardy, S., Jacques, P.E., Laflamme, L., Svotelis, A., Robert, F., and Gaudreau, L. (2009). Histone H2A.Z is essential for estrogen receptor signaling. Genes Dev. *23*, 1522-1533.

He, H.H., Meyer, C.A., Chen, M.W., Jordan, V.C., Brown, M., and Liu, X.S. (2012). Differential DNase I hypersensitivity reveals factor-dependent chromatin dynamics. Genome Res. *22*, 1015-1025.

Hurtado, A., Holmes, K.A., Ross-Innes, C.S., Schmidt, D., and Carroll, J.S. (2011). FOXA1 is a key determinant of estrogen receptor function and endocrine response. Nat. Genet. *43*, 27-33.

Jeronimo, C., Watanabe, S., Kaplan, C.D., Peterson, C.L., and Robert, F. (2015). The Histone Chaperones FACT and Spt6 Restrict H2A.Z from Intragenic Locations. Mol. Cell *58*, 1113-1123.

Jin, C., Zang, C., Wei, G., Cui, K., Peng, W., Zhao, K., and Felsenfeld, G. (2009). H3.3/H2A.Z double variant-containing nucleosomes mark 'nucleosome-free regions' of active promoters and other regulatory regions. Nat. Genet. *41*, 941-945.

Joseph, R., Orlov, Y.L., Huss, M., Sun, W., Kong, S.L., Ukil, L., Pan, Y.F., Li, G., Lim, M., Thomsen, J.S. et al. (2010). Integrative model of genomic factors for determining binding site selection by estrogen receptor-α. Mol. Syst. Biol. *6*, 456.

Karpiuk, O., Najafova, Z., Kramer, F., Hennion, M., Galonska, C., Konig, A., Snaidero, N., Vogel, T., Shchebet, A., Begus-Nahrmann, Y. et al. (2012). The histone H2B monoubiquitination regulatory pathway is required for differentiation of multipotent stem cells. Mol. Cell *46*, 705-713.

Li, W., Notani, D., Ma, Q., Tanasa, B., Nunez, E., Chen, A.Y., Merkurjev, D., Zhang, J., Ohgi, K., Song, X. et al. (2013). Functional roles of enhancer RNAs for oestrogen-dependent transcriptional activation. Nature *498*, 516-520.

Li, Z., Gadue, P., Chen, K., Jiao, Y., Tuteja, G., Schug, J., Li, W., and Kaestner, K.H. (2012). Foxa2 and H2A.Z mediate nucleosome depletion during embryonic stem cell differentiation. Cell *151*, 1608-1616.

Liu, Z., Merkurjev, D., Yang, F., Li, W., Oh, S., Friedman, M.J., Song, X., Zhang, F., Ma, Q., Ohgi, K.A. et al. (2014). Enhancer activation requires trans-recruitment of a mega transcription factor complex. Cell *159*, 358-373.

Materne, P., Vázquez, E., Sánchez, M., Yague-Sanz, C., Anandhakumar, J., Migeot, V., Antequera, F., and Hermand, D. (2016). Histone H2B ubiquitylation represses gametogenesis by opposing RSC-dependent chromatin remodeling at the ste11 master regulator locus. eLife *5*, e13500.

Minsky, N., Shema, E., Field, Y., Schuster, M., Segal, E., and Oren, M. (2008). Monoubiquitinated H2B is associated with the transcribed region of highly expressed genes in human cells. Nat. Cell Biol. *10*, 483-488.

Murray, S.C., Haenni, S., Howe, F.S., Fischl, H., Chocian, K., Nair, A., and Mellor, J. (2015). Sense and antisense transcription are associated with distinct chromatin architectures across genes. Nucleic Acids Res. *43*, 7823-7837.

Nagarajan, S., Hossan, T., Alawi, M., Najafova, Z., Indenbirken, D., Bedi, U., Taipaleenmaki, H., Ben-Batalla, I., Scheller, M., Loges, S. et al. (2014). Bromodomain protein BRD4 is required for estrogen receptor-dependent enhancer activation and gene transcription. Cell Rep. *8*, 460-469.

Obri, A., Ouararhni, K., Papin, C., Diebold, M.L., Padmanabhan, K., Marek, M., Stoll, I., Roy, L., Reilly, P.T., Mak, T.W. et al. (2014). ANP32E is a histone chaperone that removes H2A.Z from chromatin. Nature *505*, 648-653.

Papamichos-Chronakis, M., Watanabe, S., Rando, O.J., and Peterson, C.L. (2011). Global regulation of H2A.Z localization by the INO80 chromatin-remodeling enzyme is essential for genome integrity. Cell *144*, 200-213.

Pavri, R., Zhu, B., Li, G., Trojer, P., Mandal, S., Shilatifard, A., and Reinberg, D. (2006). Histone H2B monoubiquitination functions cooperatively with FACT to regulate elongation by RNA polymerase II. Cell *125*, 703-717.

Prenzel, T., Begus-Nahrmann, Y., Kramer, F., Hennion, M., Hsu, C., Gorsler, T., Hintermair, C., Eick, D., Kremmer, E., Simons, M. et al. (2011). Estrogen-

dependent gene transcription in human breast cancer cells relies upon proteasome-dependent monoubiquitination of histone H2B. Cancer Res. *71*, 5739-5753.

Schmidt, D., Wilson, M.D., Spyrou, C., Brown, G.D., Hadfield, J., and Odom, D.T. (2009). ChIP-seq: using high-throughput sequencing to discover protein-DNA interactions. Methods *48*, 240-248.

Shema, E., Tirosh, I., Aylon, Y., Huang, J., Ye, C., Moskovits, N., Raver-Shapira, N., Minsky, N., Pirngruber, J., Tarcic, G. et al. (2008). The histone H2B-specific ubiquitin ligase RNF20/hBRE1 acts as a putative tumor suppressor through selective regulation of gene expression. Genes Dev. *22*, 2664-2676.

Shimbo, T., Du, Y., Grimm, S.A., Dhasarathy, A., Mav, D., Shah, R.R., Shi, H., and Wade, P.A. (2013). MBD3 localizes at promoters, gene bodies and enhancers of active genes. PLoS Genet. *9*, e1004028.

Shlyueva, D., Stampfel, G., and Stark, A. (2014). Transcriptional enhancers: from properties to genome-wide predictions. Nat. Rev. Genet. *15*, 272-286.

Smolle, M., and Workman, J.L. (2013). Transcription-associated histone modifications and cryptic transcription. Biochim. Biophys. Acta *1829*, 84-97.

Tarcic, O., Pateras, I.S., Cooks, T., Shema, E., Kanterman, J., Ashkenazi, H., Boocholez, H., Hubert, A., Rotkopf, R., Baniyash, M. et al. (2016). RNF20 links histone H2B ubiquitylation with inflammation and inflammation-associated cancer. Cell Rep. *14*, 1462-1476.

Teves, S.S., Weber, C.M., and Henikoff, S. (2014). Transcribing through the nucleosome. Trends Biochem. Sci. *39*, 577-586.

Theodorou, V., Stark, R., Menon, S., and Carroll, J.S. (2013). GATA3 acts upstream of FOXA1 in mediating ESR1 binding by shaping enhancer accessibility. Genome Res. *23*, 12-22.

Tosi, A., Haas, C., Herzog, F., Gilmozzi, A., Berninghausen, O., Ungewickell, C., Gerhold, C.B., Lakomek, K., Aebersold, R., Beckmann, R. et al. (2013). Structure and subunit topology of the INO80 chromatin remodeler and its nucleosome complex. Cell *154*, 1207-1219.

Venkatesh, S., and Workman, J.L. (2015). Histone exchange, chromatin structure and the regulation of transcription. Nat. Rev. Mol. Cell. Biol. *16*, 178-189.

Wang, L., Du, Y., Ward, J.M., Shimbo, T., Lackford, B., Zheng, X., Miao, Y.L., Zhou, B., Han, L., Fargo, D.C. et al. (2014). INO80 facilitates pluripotency gene activation in embryonic stem cell self-renewal, reprogramming, and blastocyst development. Cell Stem Cell *14*, 575-591.

Watanabe, S., Radman-Livaja, M., Rando, O.J., and Peterson, C.L. (2013). A histone acetylation switch regulates H2A.Z deposition by the SWR-C remodeling enzyme. Science *340*, 195-199.

Weake, V.M., and Workman, J.L. (2008). Histone ubiquitination: triggering gene activity. Mol. Cell *29*, 653-663.

Yao, T., Song, L., Jin, J., Cai, Y., Takahashi, H., Swanson, S.K., Washburn, M.P., Florens, L., Conaway, R.C., Cohen, R.E. et al. (2008). Distinct modes of regulation of the Uch37 deubiquitinating enzyme in the proteasome and in the Ino80 chromatin-remodeling complex. Mol. Cell *31*, 909-917.

Yen, K., Vinayachandran, V., and Pugh, B.F. (2013). SWR-C and INO80 chromatin remodelers recognize nucleosome-free regions near +1 nucleosomes. Cell *154*, 1246-1256.

Zentner, G.E., and Henikoff, S. (2013). Regulation of nucleosome dynamics by histone modifications. Nat. Struct. Mol. Biol. *20*, 259-266.

Zhang, X.Y., Varthi, M., Sykes, S.M., Phillips, C., Warzecha, C., Zhu, W., Wyce, A., Thorne, A.W., Berger, S.L., and McMahon, S.B. (2008). The putative cancer stem cell marker USP22 is a subunit of the human SAGA complex required for activated transcription and cell-cycle progression. Mol. Cell *29*, 102-111.

Zhao, Y., Lang, G., Ito, S., Bonnet, J., Metzger, E., Sawatsubashi, S., Suzuki, E., Le Guezennec, X., Stunnenberg, H.G., Krasnov, A. et al. (2008). A TFTC/STAGA module mediates histone H2A and H2B deubiquitination, coactivates nuclear receptors, and counteracts heterochromatin silencing. Mol. Cell *29*, 92-101.

Zhou, L., Holt, M.T., Ohashi, N., Zhao, A., Muller, M.M., Wang, B., and Muir, T.W. (2016). Evidence that ubiquitylated H2B corrals hDot1L on the nucleosomal surface to induce H3K79 methylation. Nat. Commun. *7*, 10589.

Zhu, B., Zheng, Y., Pham, A.D., Mandal, S.S., Erdjument-Bromage, H., Tempst, P., and Reinberg, D. (2005). Monoubiquitination of human histone H2B: the factors involved and their roles in HOX gene regulation. Mol. Cell *20*, 601-611.

Zofall, M., Fischer, T., Zhang, K., Zhou, M., Cui, B., Veenstra, T.D., and Grewal, S.I. (2009). Histone H2A.Z cooperates with RNAi and heterochromatin factors to suppress antisense RNAs. Nature *461*, 419-422.

FIGURE LEGENDS

Figure 1. H2B monoubiquitination enzymes RNF20/RNF40 downregulate inducible transcriptional activity through enhancer regulation.

(A) Schematic representation of the luciferase reporter constructs used for the experiments of Figure 1B-1D and Figure 1F-1G.

(B-E) Luciferase reporter assays in HEK293T cells with (B-D) or without (E, bottom panel) the corresponding nuclear receptor-dependent enhancer constructs upon overexpression of RNF20, RNF40 or both. Cells were treated with vehicle alone (Control) or with 17β-estradiol (E2; B), dexamethasone (Dex; C) or progesterone (P4; D).

(F and G) Luciferase reporter gene assays with ERα-dependent enhancer construct in HEK293T (F) or breast cancer cells (MDA-MB134; G) infected with lentiviral shRNA constructs against RNF20, RNF40 or both. A scrambled shRNA (shSC) and an shRNA targeting the bacterial β-galactosidase (shLacZ) were used as negative controls.

(H) Immunoblot showing the levels of ERα protein and monoubiquitination of histone H2B (H2Bub1) in MDA-MB134 cells infected with the indicated shRNA constructs. the H2Bub1/H2B ratios indicated below the image were determined with the software ImageJ.

(I and J) Luciferase reporter assays with a Gal4-dependent enhancer construct in HEK293T cells infected with the indicated shRNA constructs. Chimeric proteins with the Gal4 DNA binding domain fused to the N-terminal domain of ERα carrying the constitutively active activation function 1 (I) or to the ligand binding domain of ERα with the ligand-inducible activation function 2 (J) were used to assess the effect of

H2B monoubiquitination on constitutive or inducible transcriptional activity, respectively.

(K) Luciferase reporter assays with an ERα-dependent enhancer in HEK293T cells overexpressing Flag-tagged RNF20 and RNF40 along with wild-type H2B (H2Bwt) or the H2B mutant K120/125R (H2Bmut).

(B-G and I-K) RLU, relative luciferase units. Relevant statistically significant values, determined as indicated in Experimental procedures, are highlighted by asterisks (* $p<0.01$; ** $p<0.0001$). An empty vector was transfected as a negative control for overexpression experiments.

See also Figures S1A-S1K.

Figure 2. Impairment of histone H2B monoubiquitination increases endogenous enhancer activity and target gene expression.

(A-F) qPCR quantification of the expression of ERα target genes in MDA-MB134 cells infected with shRNA constructs as indicated. mRNA levels are expressed relative to the shSC control condition.

(G, H, J and K) Quantification by qPCR of the enhancer RNAs (eRNAs) of the *GREB1* (G and H) and *TFF1* (J and K) enhancers in shRNA-infected MDA-MB134 cells. eRNA levels are expressed relative to the shSC control condition.

(I and L) Chromatin immunoprecipitation followed by qPCR (ChIP-qPCR) of ERα on the *GREB1* (I) and *TFF1* (L) enhancers in shRNA-infected MDA-MB134 cells. ERα ChIP-qPCR values are standardized to the first intron of *c-MYC*.

See also Figures S2A to S2C.

Figure 3. Monoubiquitination of histone H2B drops at active enhancers and accessible chromatin regions.

(A) Genomic profiles of H2Bub1, ERα, Med1, P300 and DNase I hypersensitivity (DNase-seq) over the 5' regions of two E2-induced genes.

(B) Aggregate plot analyses of H2Bub1 in confidence level-based groups (high, medium and low) of ERα binding sites (ERBS) in MCF-7 cells treated with vehicle alone (top panel) or E2 (bottom panel). "High" ERBS comprised 1067 sites defined as having a confidence level ($-10*\log_{10}$ p-value) in ERα ChIP-seq data of more than 150; "Medium" ERBS (4149 sites) are between 50 and 150; "Low" ERBS (10558 sites) are less than 50.

(C and D) Aggregate plots of H2Bub1 associated with low ERBS or high ERBS (asterisks indicate p-value<0.00001 between vehicle and E2 conditions at the center).

(E) Kinetic analysis of H2Bub1 by ChIP-qPCR on the center of the *GREB1* (black circles) and *TFF1* (red squares) enhancers at different time points after E2 treatment of MDA-MB134 cells. For these ChIP experiments, MNase digestion was used instead of sonication, and the ChIP-qPCR values for H2Bub1 were normalized to those of H2B (H2Bub1/H2B). Values are represented as fold of control (untreated cells).

(F-H) Aggregate plot analyses of H2Bub1 at Med1 and P300 binding sites, and at DNase hypersensitive sites (DHS) with the indicated treatments.

(I and J) Aggregate plot analyses of DNase-seq (I, chromatin accessibility) and MNase-seq (J, nucleosome occupancy) signals over regions containing H2Bub1 peaks or valleys (defined and extracted as indicated in Experimental procedures). The reanalyses of ChIP-seq data were performed on the publicly available datasets

with the GEO accession numbers GSE55921 (H2Bub1 and ERα), GSE60270 (Med1, P300), GSE33216 (DNase-seq) and GSE51097 (MNase-seq).

See also Figures S3A-S3J.

Figure 4. Histone H2B monoubiquitination controls the occupancy of histone H2A.Z at active enhancers.

(A) Aggregate plot analysis of H2A.Z in confidence level-based groups (high, medium and low) of ERα binding sites (ERBS) in MCF-7 cells treated with vehicle (see legend of Figure 3B).

(B) Aggregate plot of H2Bub1 at H2A.Z binding sites in MCF-7 cells with the indicated treatments.

(C) Scatterplot comparing the mean of the H2A.Z and H2Bub1 signals on high ERBS. The coefficient of determination (r^2) and p-value of the linear regression are indicated and the dense area of dots was arbitrarily stained in grey for clarity.

(D) ChIP-qPCR kinetics of ERα (dotted lines) and H2A.Z (full lines) on the *GREB1* (black) and *TFF1* (red) enhancers at different times after E2 treatment of MDA-MB134 cells. The ChIP-qPCR values of H2A.Z were normalized to those of H4 (H2A.Z/H4). Values are represented as fold of control (untreated cells).

(E and F) Impact of the knock-down of RNF40 on the levels of H2A.Z at the *GREB1* (E) and *TFF1* (F) enhancers. MDA-MB134 cells were infected with the indicated shRNA constructs. H2A.Z/H4 ChIP-qPCR values are represented as fold of the shSC control.

(G) ChIP-qPCR of H2A.Z on the *GREB1* and *TFF1* enhancers in MDA-MB134 cells overexpressing either wild-type H2B (H2Bwt, black bars) or the H2B mutant

K120/125R (H2Bmut, white bars). H2A.Z/H4 ChIP-qPCR values are represented as fold of H2Bwt.

(H) ChIP-qPCR of H2A.Z on the ERα-dependent enhancer of the transfected reporter plasmid upon overexpression of RNF20 and RNF40 in HEK293T cells. H2A.Z/H4 ChIP-qPCR values are represented as fold of empty vector control.

(I) Immunoblot of the immunoprecipitation of Flag-tagged H2B (Flag IP) expressed in HE293T cells, with or without co-overexpression of RNF20/40. The blot was probed with antibodies to H2A.Z or Flag. A control immunoprecipitation was performed in parallel with a control IgG (Ctrl IP).

(J and K) Impact of the knock-down of RNF20/40 on antisense RNAs over the *GREB1* (J) and *TFF1* (K) gene bodies. MDA-MB134 cells were infected with the indicated shRNA constructs. Antisense RNA levels are represented as fold of the shSC control. An empty vector was transfected as a negative control for RNF20/40 overexpression experiments (H and I). Both shSC- and shLacZ-infected MDA-MB134 cells were used as negative controls (E, F, J and K). Datasets GSE55921 (H2Bub1 and ERα) and GSE57436 (H2A.Z) were used (A-C).

See also Figures S4A-S4G.

Figure 5. Recruitment of the histone H2A.Z remodeler INO80 to inducible enhancers is impaired by H2B monoubiquitination.

(A) Combined interactome of RNF20 and RNF40 generated with Cytoscape using the PPiMapBuilder plug-in. Two interactors of interest are highlighted in yellow and interactions between them are in red. Note that ESR1 is the official name of ERα.

(B) The knockdowns of RNF20 or RNF40 affect H2Bub1 but not INO80 levels. Protein extracts were made from MDA-MB134 cells and HEK293T cells infected with

the indicated shRNA constructs. Immunoblotting was performed for INO80, H2Bub1, H2B and GAPDH, and H2Bub1 levels relative to H2B levels were determined with the software ImageJ.

(C) The INO80 interaction with ERα and RNF40 is stimulated by E2. Immunoprecipitation of ERα, RNF20, RNF40 or INO80 from extracts of MDA-MB134 cells treated with vehicle (-) or E2 (+; where indicated), followed by immunoblotting. A control immunoprecipitation was performed in parallel with a control IgG.

(D) Quantification by qPCR of the eRNAs of the *GREB1* and *TFF1* enhancers in MDA-MB134 cells infected with the indicated shRNA constructs. eRNA levels are relative to the shSC control condition.

(E and F) Luciferase reporter gene assays of an ERα-dependent enhancer in HEK293T cells infected with the indicated shRNA constructs. RLU, relative luciferase activities. Relevant statistically significant values are highlighted by asterisks (* $p<0.05$).

(G) ChIP-qPCR of INO80 on the *GREB1* and *TFF1* enhancers with MDA-MB134 cells infected with the indicated shRNA constructs. INO80 ChIP-qPCR values are standardized to the GAPDH internal standard.

(H) ChIP-qPCR of INO80 on the *GREB1* and *TFF1* enhancers with MDA-MB134 cells overexpressing either wild-type H2B (H2Bwt, black bars) or the H2B mutant K120/125R (H2Bmut, white bars). INO80 ChIP-qPCR values are represented as fold of H2Bwt.

(I) ChIP-qPCR of INO80 on the ERα-dependent enhancer of the transfected reporter plasmid upon overexpression of RNF20/40 in HEK293T cells. INO80 ChIP-qPCR values are represented as fold of empty vector control.

(J) Immunoprecipitation of Flag-tagged H2B (Flag IP) followed by immunoblotting of INO80 or Flag performed with extracts of HEK293T cells transfected with either Flag-tagged H2Bwt or H2Bmut and overexpressing RNF20/40. Co-immunoprecipitated INO80 levels were normalized to total INO80 levels and expressed as a ratio relative to immunoprecipitated Flag-H2B. A control immunoprecipitation was performed in parallel with a control IgG (Ctrl IP).

An empty vector was transfected as a negative control for RNF20/40 overexpression experiments (I and J).

shSC- and shLacZ-infected cells were used as negative controls (B, D, E, F and G).

See also Figures S5A-S5C.

Figure 6. Schematic representation of the model. It depicts the proposed mechanism of the regulation of inducible enhancers by H2B monoubiquitination through the inhibition of the eviction of H2A.Z by INO80.

Figure 1

Click here to download Figure Figure1.tif

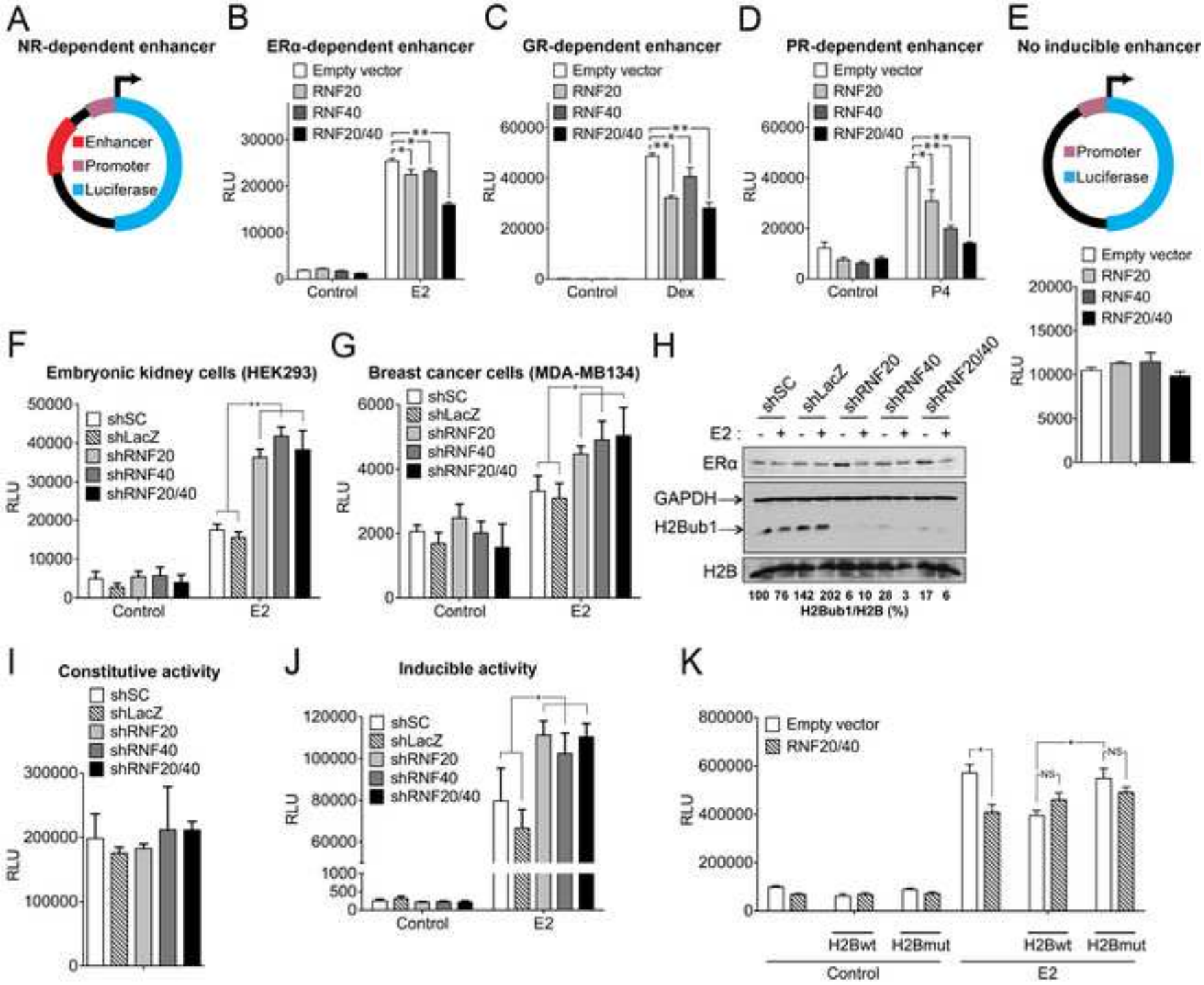

Figure 2

Click here to download Figure Figure2.tif

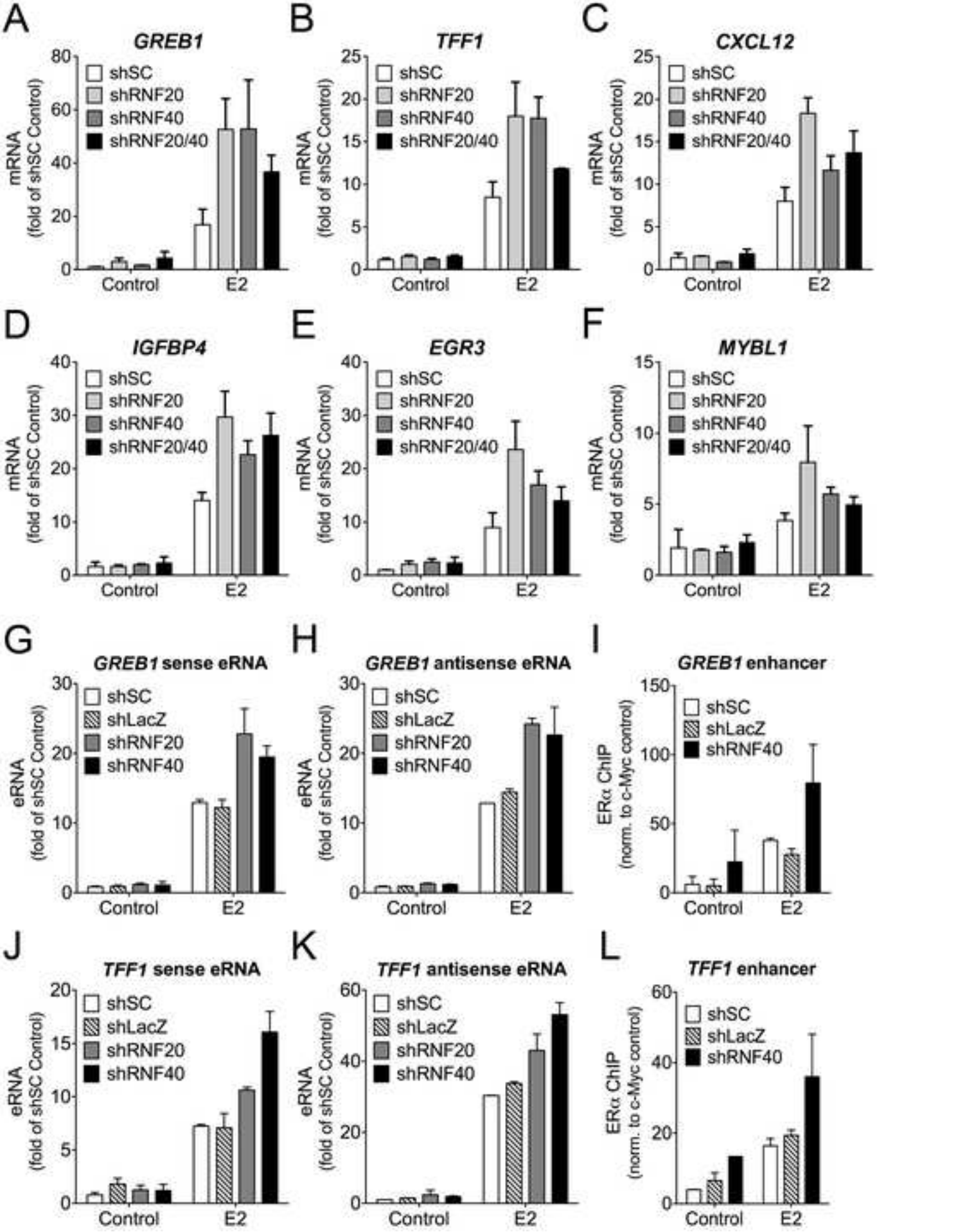

Figure 3

Click here to download Figure Figure3.tif

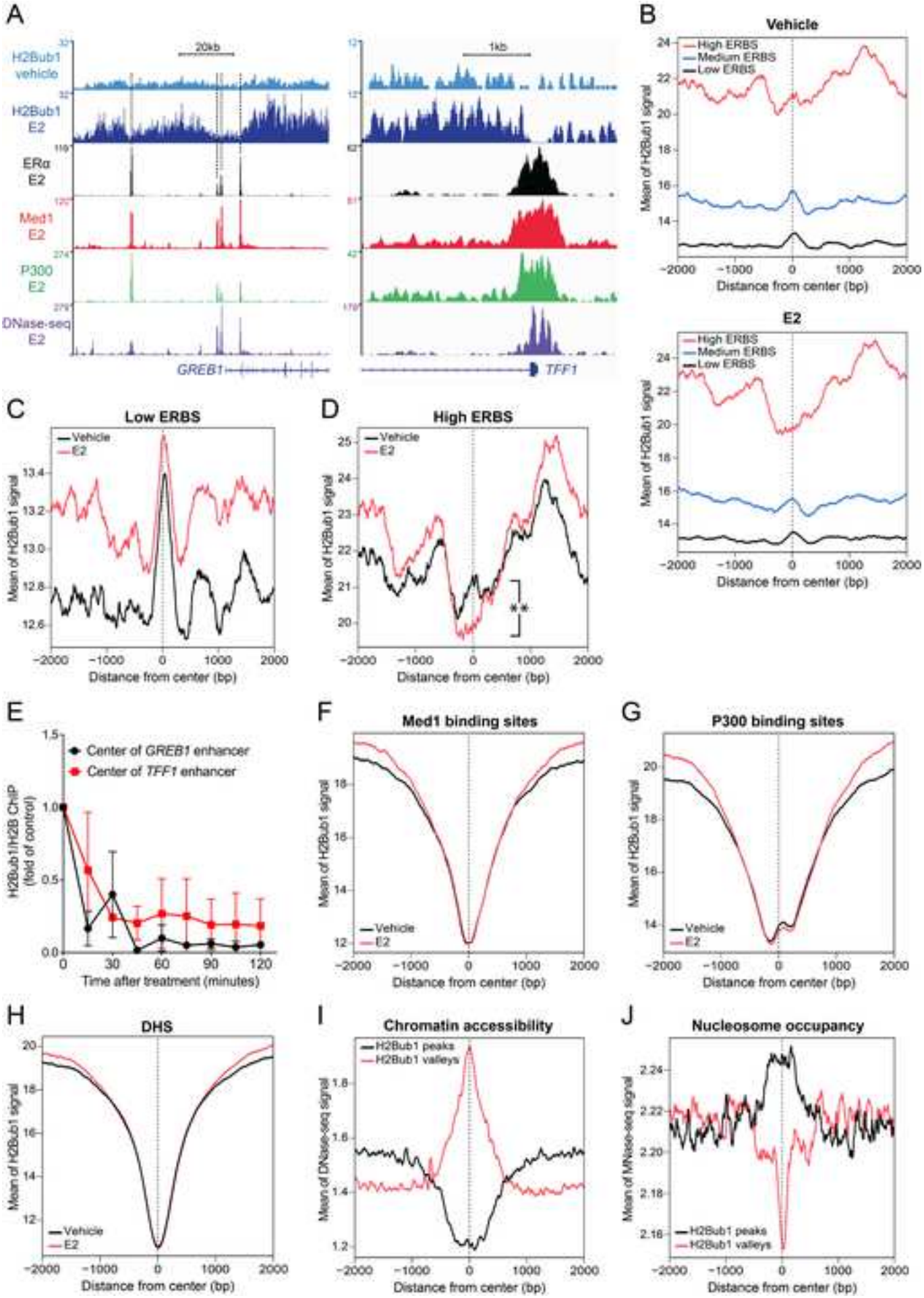

Figure 4

Click here to download Figure Figure4.tif

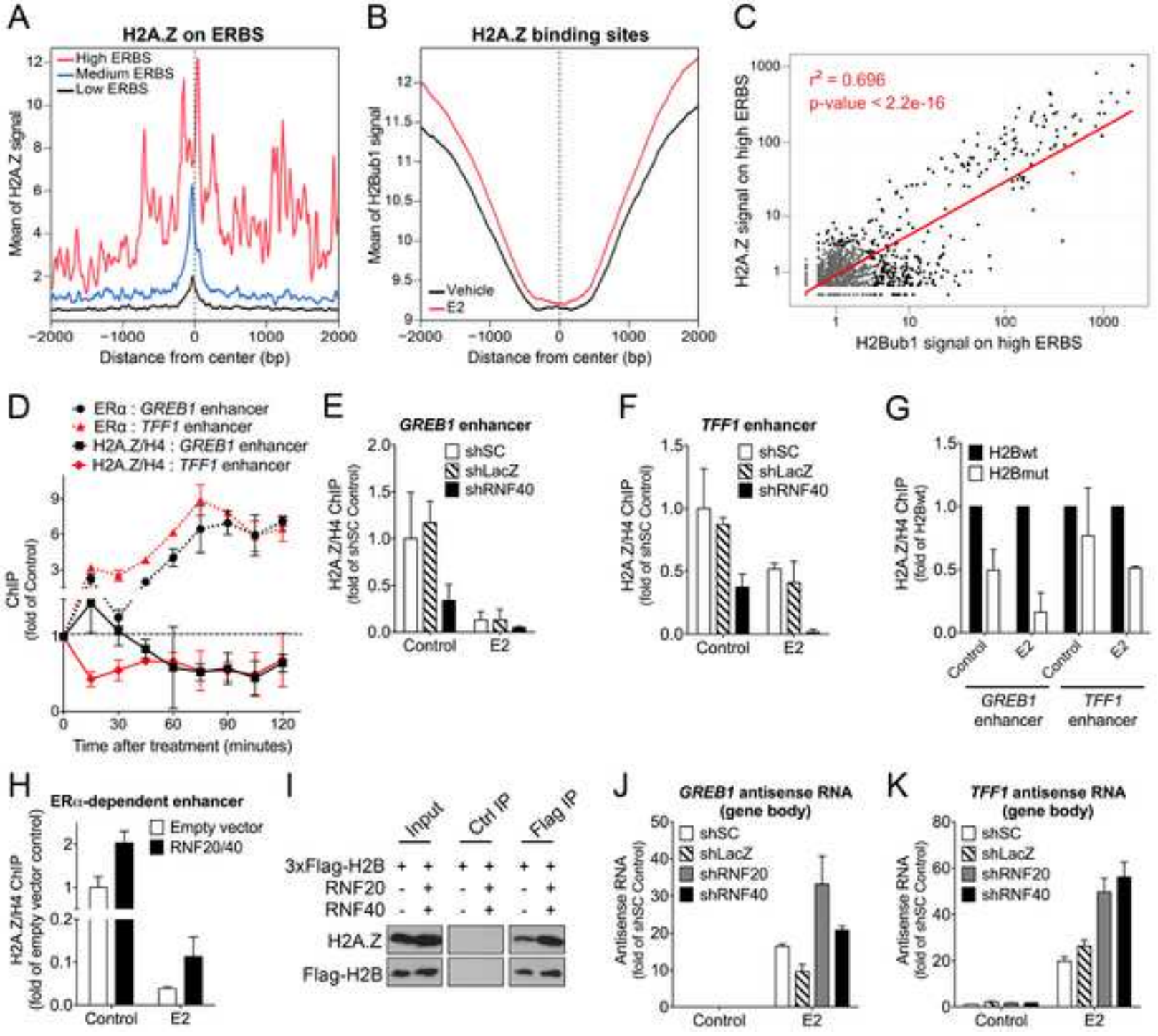

Figure 5

Click here to download Figure Figure5.tif

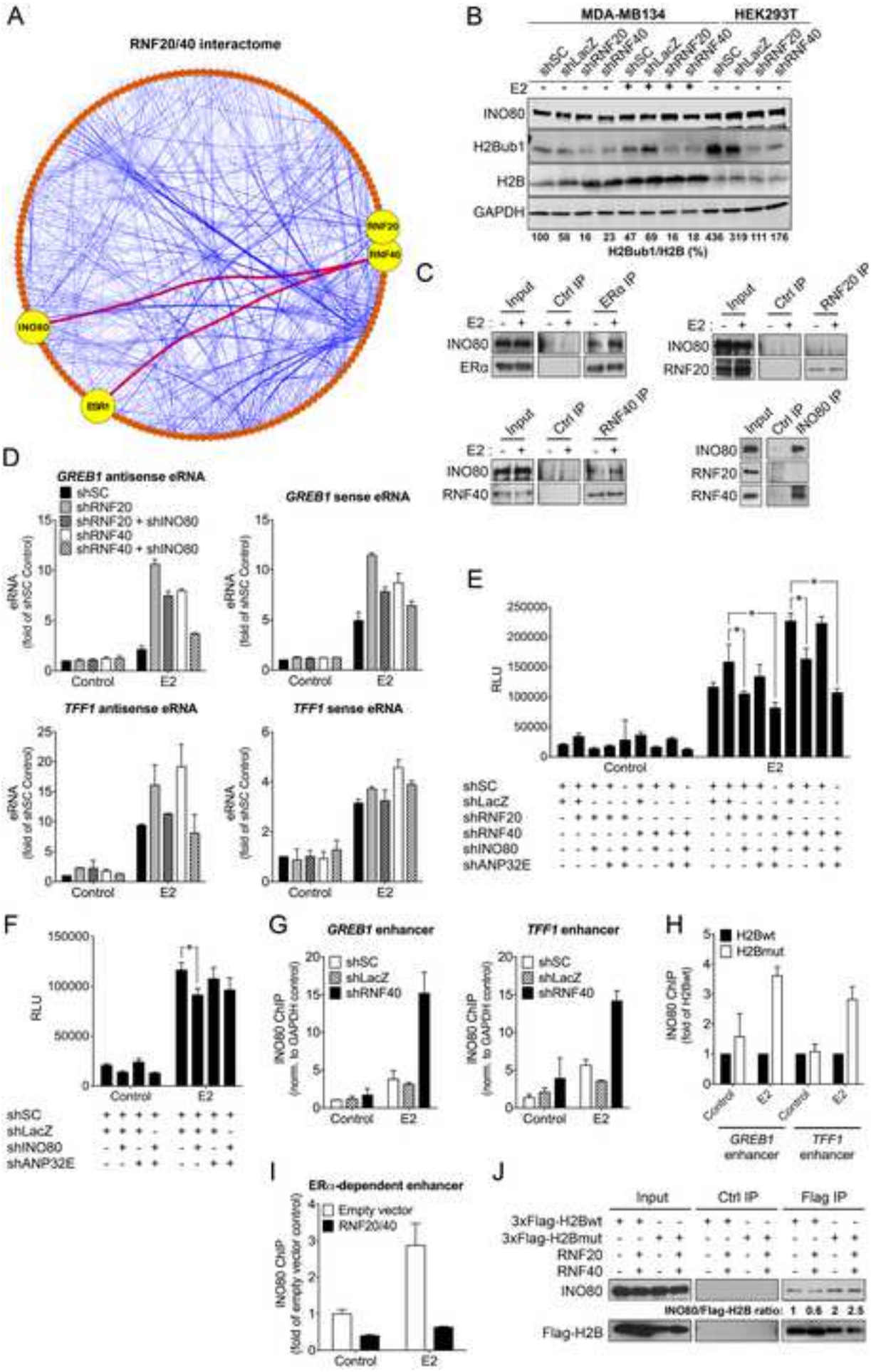

Figure 6

Click here to download Figure Figure6.tif

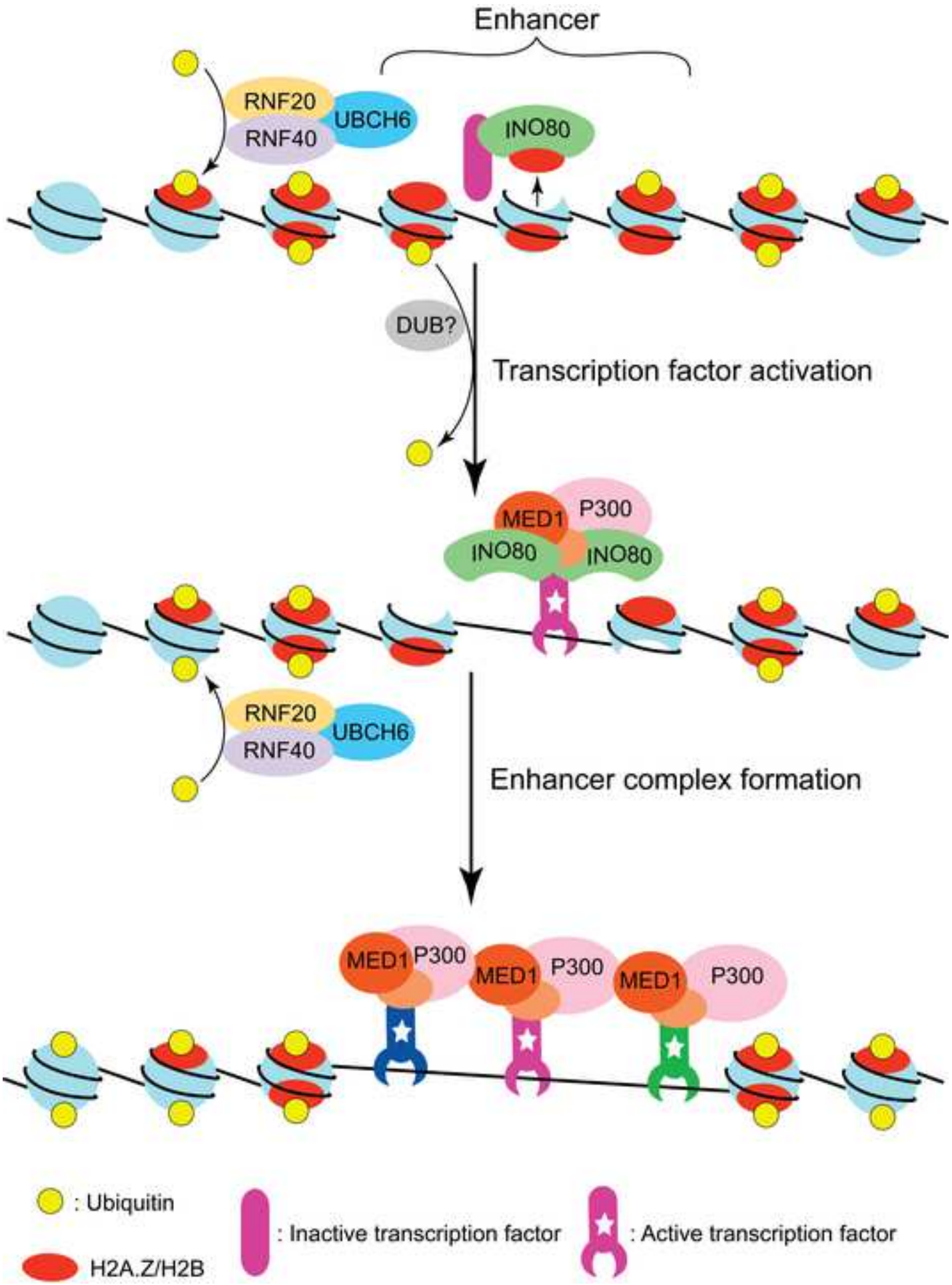

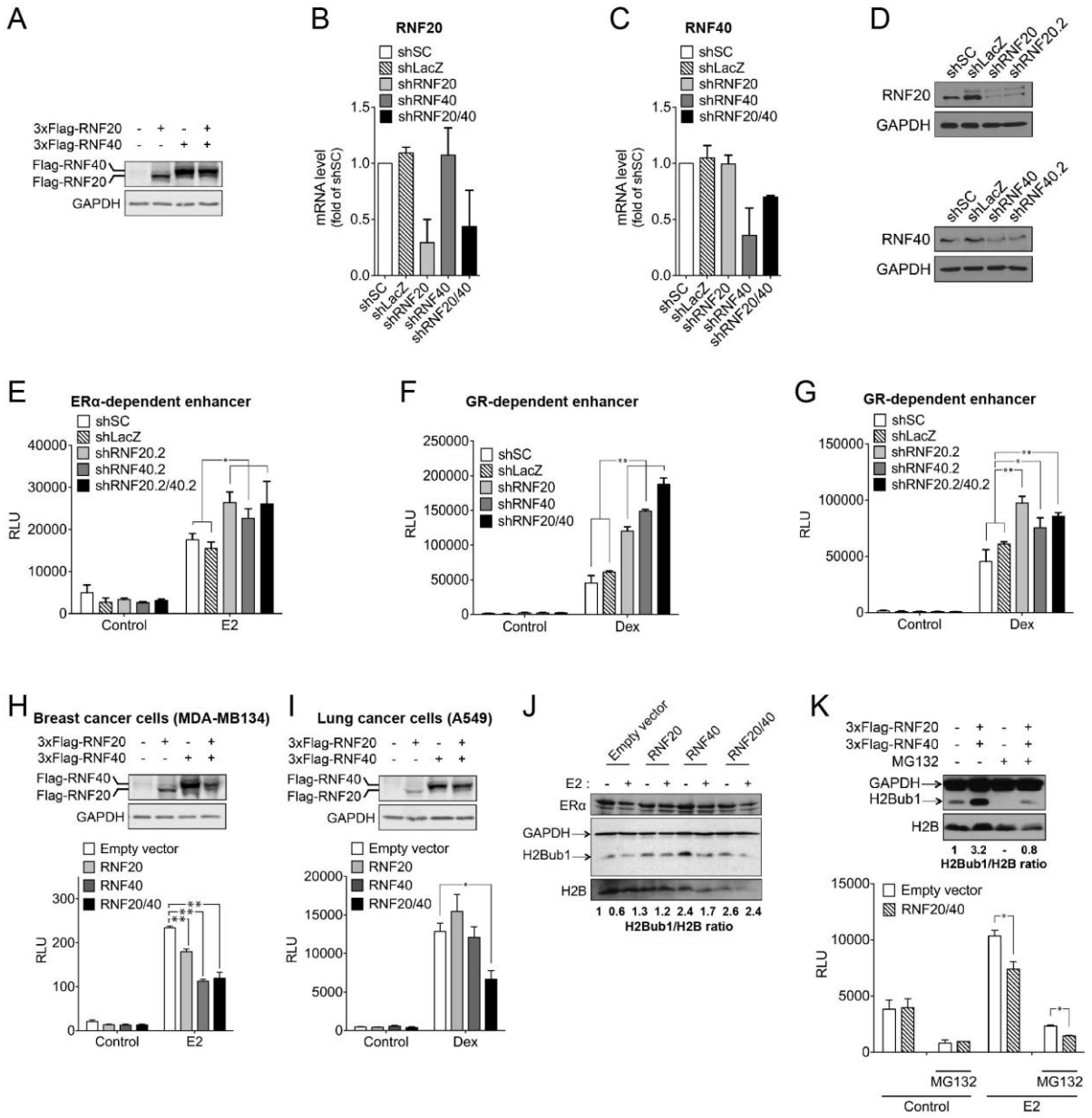

Figure S1 – related to Figure 1.
(A) Representative immunoblot of the experiments shown in Figures 1B-1E of Flag-tagged RNF20 and RNF40 overexpressed in HEK293T cells.
(B and C) Quantification by qPCR of the knockdown efficiency and specificity of the indicated shRNA constructs targeting RNF20 (B) or RNF40 expression (C).
(D) Representative immunoblot of the knockdowns of RNF20 (top panel) or RNF40 (bottom panel) by two different shRNAs constructs in HEK293T cells.
(E-G) Luciferase reporter assays with an ERα-dependent enhancer (E) or a GR-dependent enhancer (F and G) in HEK293T infected with the indicated shRNA constructs.
(H and I) Luciferase reporter assays with an ERα-dependent enhancer in MDA-MB134 cells (H, bottom panel) or a GR-dependent enhancer in A549 cells (I, bottom panel). Both cell lines were transfected to overexpress Flag-tagged RNF20 and RNF40 and a representative immunoblot is shown for each one (H and I, top panels).
(J) Immunoblot showing the ERα protein levels and the monoubiquitination of histone H2B (H2Bub1) in MDA-MB134 cells overexpressing Flag-tagged RNF20 and RNF40 and treated with only vehicle (-) or E2 (+). H2Bub1 levels relative to H2B levels were determined with the software ImageJ.
(K) Effect of inhibition of the proteasome. Immunoblot (top panel) showing the representative levels of H2Bub1 relative to H2B of the experiment shown in the bottom panel. Luciferase reporter assays with an ERα-dependent

enhancer in HEK293T cells overexpressing Flag-tagged RNF20 and RNF40 treated or not with the proteasome inhibitor MG132 (bottom panel).
An empty vector was transfected as a negative control for overexpression experiments. A scrambled shRNA (shSC) and an shRNA targeting the bacterial β-galactosidase (shLacZ) were used as negative controls for experiments involving shRNA constructs. Relevant statistically significant values, determined as indicated in Experimental procedures, are highlighted by asterisks (* $p<0.01$; ** $p<0.0001$).

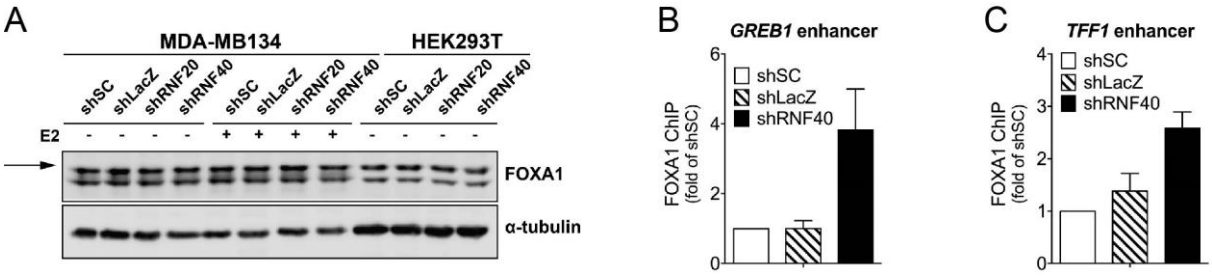

Figure S2 – related to Figure 2.
(A) Knockdown of RNF20 or RNF40 does not affect FOXA1 protein levels. Protein extracts were made from MDA-MB134 and HEK293T cells infected with the indicated shRNA constructs. Immunoblotting was performed for FOXA1 (arrow) and α-tubulin.
(B and C) ChIP-qPCR of FOXA1 on the *GREB1* (B) and *TFF1* (C) enhancers in MDA-MB134 cells infected with the indicated shRNA constructs. ChIP-qPCR values are represented as fold of the shSC value set to 1. Standardization was performed with the first intron of *c-MYC*. shSC and shLacZ were used as negative controls.

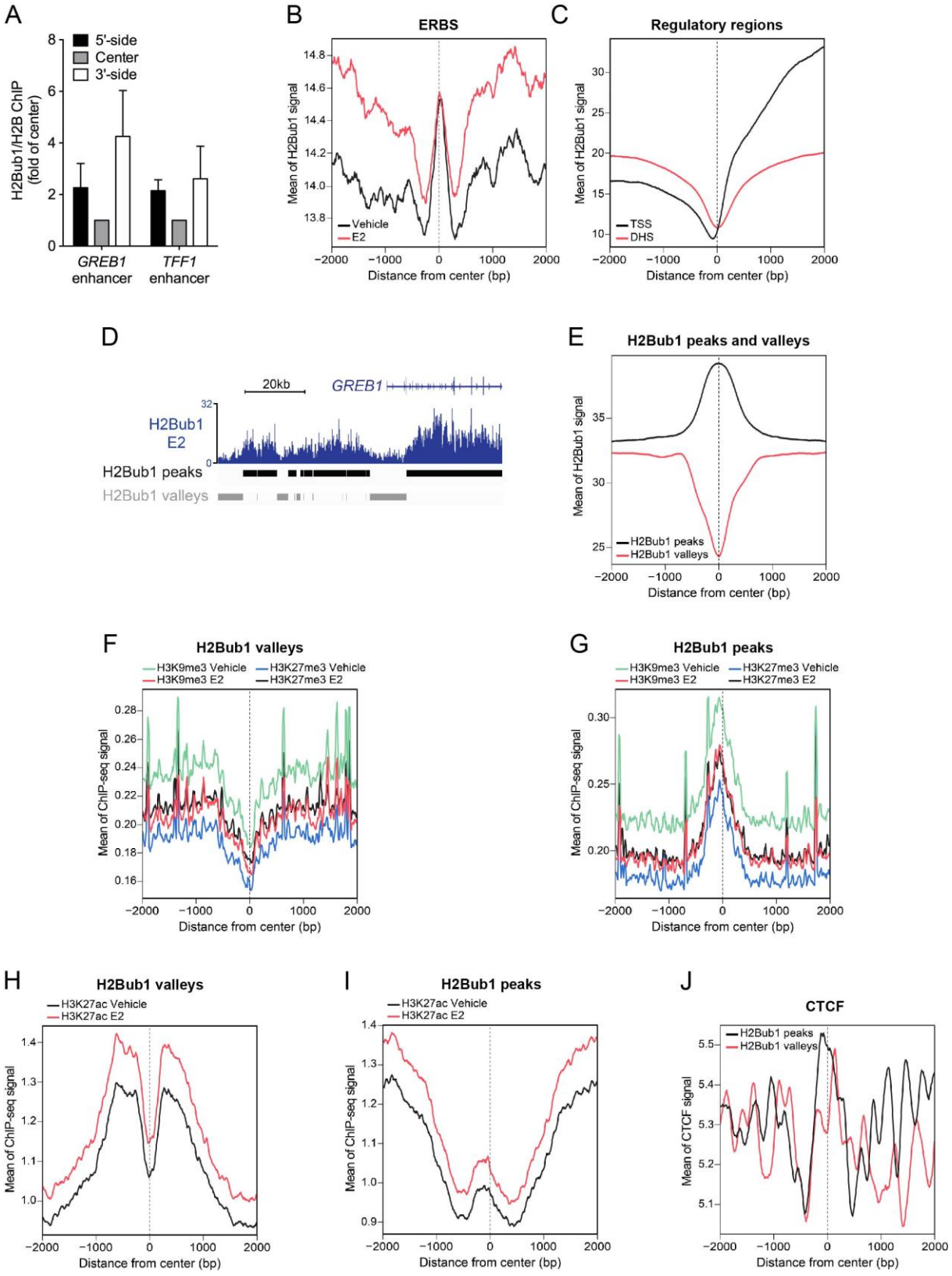

Figure S3 – related to Figure 3.
(A) ChIP-qPCR of H2Bub1 on the 5'-sides, centers and 3'-sides of the *GREB1* and *TFF1* enhancers. For these ChIP experiments with MDA-MB134 cells, MNase digestion was used instead of sonication and the ChIP-qPCR values of H2Bub1 were normalized to those of H2B (H2Bub1/H2B). Values are represented as fold of the values at the centers.

(B) Aggregate plot of H2Bub1 on ERBS in MCF-7 cells with the indicated treatments.
(C) Aggregate plot of H2Bub1 on transcription start sites (TSS) and DNase hypersensitive sites (DHS) in MCF-7 cells.
(D) Genomic binding profiles of H2Bub1 in MCF-7 cells treated with E2 on the 5'-flanking region of the *GREB1* gene with the positions of the peaks called with MACS for H2Bub1 and the positions of H2Bub1 valleys defined as the gaps between peaks.
(E) Aggregate plots of H2Bub1 peaks and valleys defined in Experimental procedures.
(F-J) Aggregate plot analyses of H3K9me3 (F and G), H3K27me3 (F and G), H3K27ac (H and I) or CTCF (J) on H2Bub1 valleys (F, H and J) or H2Bub1 peaks (G, I and J) in MCF-7 cells treated with only vehicle (F-I) or E2 (F-J).
ChIP-seq reanalyses were performed on publicly available datasets with the accession numbers GSE55921 (H2Bub1 and ERα), GSE33216 (DNase-seq), RefGene hg19 TSS, GSE23701 (H3K9me3 and H3K27me3), GSE40129 (H3K27ac) and GSE33213 (CTCF). See Experimental procedures for the references of these datasets.

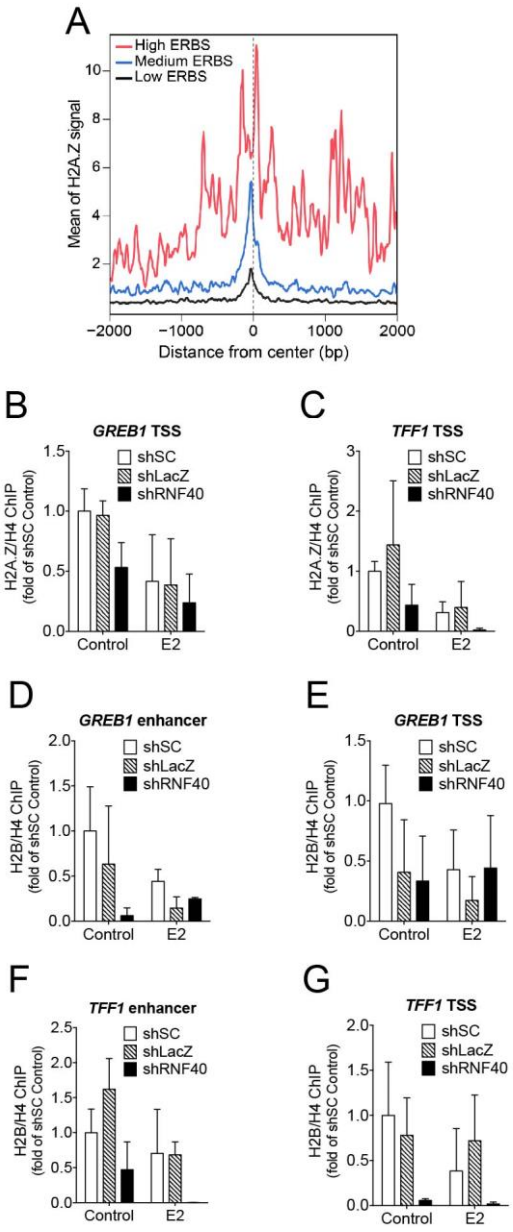

Figure S4 – related to Figure 4.
(A) Aggregate plot analysis of H2A.Z in confidence level-based groups (high, medium and low) of ERα binding sites (ERBS) in MCF-7 cells treated with E2 (see Figure 3B).
(B and C) ChIP-qPCR of H2A.Z/H4 at the *GREB1* (B) or *TFF1* (C) transcription start sites (TSS) in MDA-MB134 cells infected with the indicated shRNA constructs and treated with vehicle or E2 for 90 minutes.
(D-G) ChIP-qPCR of H2B/H4 at *GREB1* (D and E) or *TFF1* (F and G) enhancers (D and F) or TSS (E and G) in MDA-MB134 cells infected with the indicated shRNA constructs treated with vehicle or E2 for 90 minutes.
H2A.Z or H2B ChIP-qPCR values are normalized to H4 ChIP-qPCR values and represented as fold of the shSC control.
MDA-MB134 cells infected with shSC and shLacZ were used as negative controls (B-G).

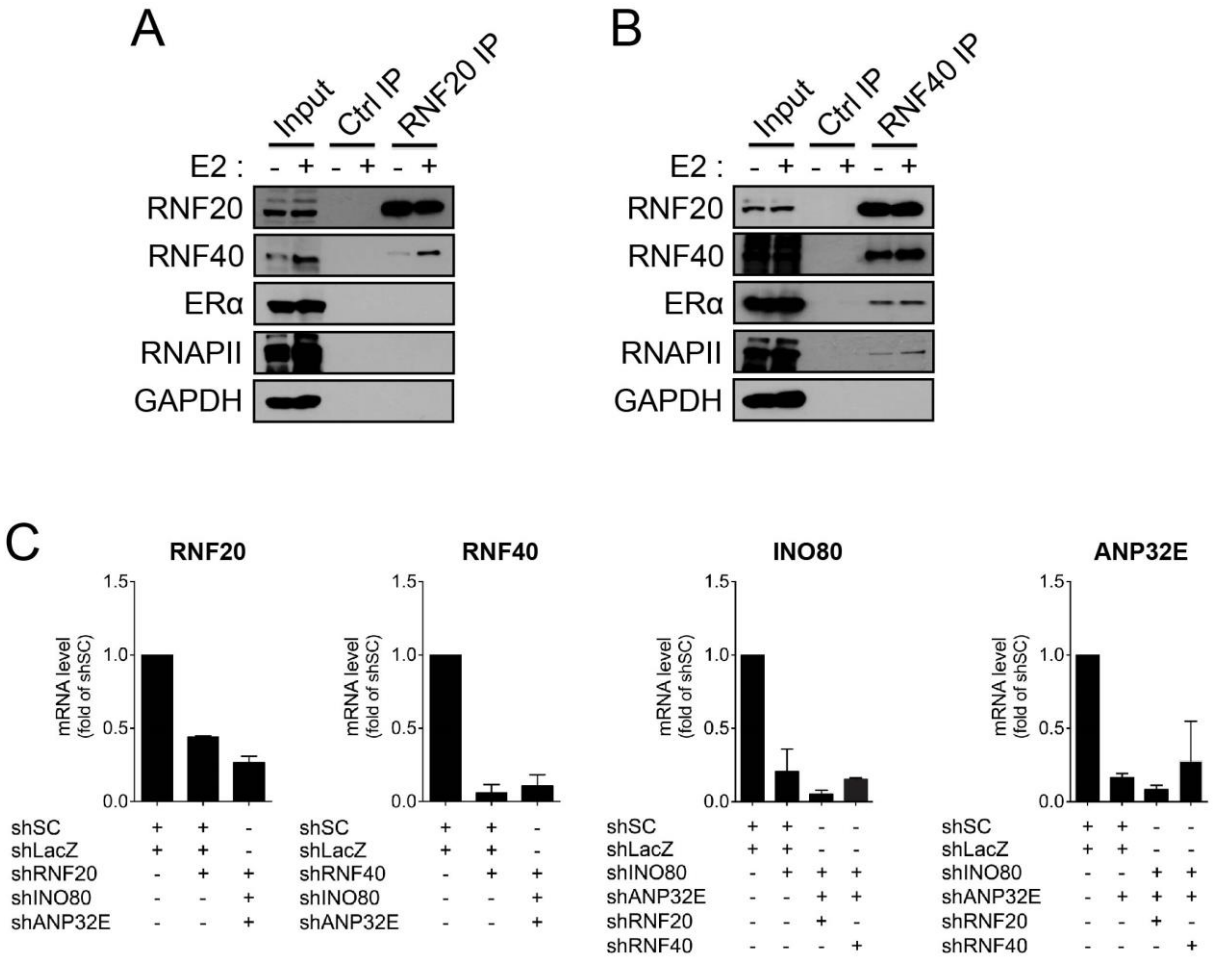

Figure S5 – related to Figure 5.
(A and B) RNF40 interacts with ERα and RNA polymerase II in an E2-independent manner. Immunoprecipitation of RNF20 (A) or RNF40 (B) followed by immunoblotting of RNF20, RNF40, ERα, RNA polymerase II (RNAPII) or GAPDH in MDA-MB134 cells treated with vehicle (–) or E2 (+). A control immunoprecipitation was performed in parallel with an anti-IgG antibody.
(C) Quantification by qPCR of the knockdown efficiencies of the indicated different combinations of shRNA constructs related to Figure 5E and 5F. mRNA levels are represented as fold of the shSC condition. Cells infected by a combination of shSC and shLacZ were used as a negative control.

Table S1 related to Experimental procedures
Primer sequences

mRNA	***Forward primer 5'-3'***	***Reverse primer 5'-3'***
RNF20	CAGGAGAATATGAGGCTACAGGA	GACAGACACTCGTGATTCGGC
RNF40	CGGGTGGAGGAACTCTGTC	CTGCCGATGTCACTTTATCCTG
GREB1	ATATGCAAGGCCAAGCCAGT	CTCGTATGCCCGTGAGACAG
TFF1	ATGGAGAACAAGGTGATCTG	ACCACAATTCTGTCTTTCAC
CXCL12	AACACTCCAAACTGTGCCCT	AGTGGGTCTAGCGGAAAGTC
IGFBP4	CACACTGATGCACGGGCAAG	CAGGGGCTGAAGCTGTTGTT
EGR3	CCGGTGACCATGAGCAGTTTG	GTTGGGCTTCTCGTTGGTCA
MYBL1	ATGTTCAGCCTACTTCTGCCTTT	CCAGACCAGCTAGAAAAACTTCC
INO80	TGGCTAAAGAGCATTCTGCTAAG	TGTGTAGTCGAAGCATGTTGTG
ANP32E	AATTTCTGAGTATGGCTAATGTGGA	ATTTCTCTGCCAGGACTTCCAA
GAPDH	GCACAACAGGAAGAGAGAGACC	AGGGGAGATTCAGTGTGGTG
ChIP	***Forward primer 5'-3'***	***Reverse primer 5'-3'***
GREB1 **enhancer -2 kb**	GAAGGGCAGAGCTGATAACG	GACCCAGTTGCCACACTTTT
TFF1 **enhancer -0.5 kb**	CACCCCGTGAGCCACTGT	CTGCAGAAGTGATTCATAGTGAGAGAT
GREB1 **TSS**	TAAATACTGCAGTAGAGATGG	GAGCTGCAAGCCTTCCATTG
TFF1 **TSS**	GCTCTTTAAGCAAACAGAGC	TCTCTGCTCCAAAGGCGACC
c-Myc **intron**	TGGCCCTTGATACTGGAGTC	GACATCCAAGGCAAGATGGT
GREB1 **enhancer 5'-side**	GCTGCTCAGCCTAAAAATGCT	TTGTCCAGCCAATCCACCAG
GREB1 **enhancer center**	AGGTTCATTACGAACTTTAGCAGT	TTGGTTGCTTCTAGGTCAGAATG
GREB1 **enhancer 3'-side**	AGTTAGCAATTTACAGCACAGTTGA	GGTACTTGCCTCTAAGAATTCAAGG
TFF1 **enhancer 5'-side**	TCCAAGAGCCCCCATTTTGAT	CCAGGGTGGTGCTCATAGTG
TFF1 **enhancer center**	Same as for *TFF1* enhancer -0.5 kb	Same as for *TFF1* enhancer -0.5 kb
TFF1 **enhancer 3'-side**	GCAATGGGTTTCCACCTCCT	CACCAGGTGAAGATGGAGCC
ERα-dependent enhancer of reporter plasmid	TCCGAGGTCCACTTCGCATA	CGCTGTTGACGCTGTTAAGC
eRNA	***Forward primer 5'-3'***	***Reverse primer 5'-3'***
GREB1 **as**	ATGTGAATGATACCGCTTTCTCT	GCATATTCAAATGACAGAAAGTACG
GREB1 **s**	AGCCAGTAGATACCAGGCAC	CTCCCATTAGTTTGGAGTTGCC
TFF1 **as**	AGAGGGGCTGCAGAAATGTA	TGAGAAATTAGGCCCTGAGGA
TFF1 **s**	GGATTAAGGTCAGGTTGGAGGA	ACGACATGTGGTGAGGTCAT
antisense RNA	***Forward primer 5'-3'***	***Reverse primer 5'-3'***
GREB1	CCTGCACAGAGGCAGTCTTT	AGCCACCAAAGGAGTTAGGC
TFF1	TTTGTGTGCATGAGAAGTGGG	TGACTTCTCTGGTTTTAATTTCTGG

Table S2 related to Experimental procedures
shRNA constructs with expression vector pLKO.1

shRNA	*Target sequence 5'-3'*	*TRCN* / reference / design tool***
shSC	CCTAAGGTTAAGTCGCCCTCG	(Sarbassov et al., 2005)
shLacZ	CGCTAAATACTGGCAGGCGTT	(Rosenbluh et al., 2012)
shRNF20	CCCTTTGTCTTCTAATGAATT	http://sirna.wi.mit.edu
shRNF20.2	GACAGTTTATCAGTCAACTTT	http://sirna.wi.mit.edu
shRNF40	GCTGTTAATTGTGATGAATTT	http://sirna.wi.mit.edu
shRNF40.2	TTCTGTTCCTGCATGTCCTCA	http://sirna.wi.mit.edu
shINO80	GGATCCCTTAATACAAGTTAA	TRCN0000365460
shANP32E	GTATGGCTAATGTGGAACTAA	TRCN0000077935

* TRCN, the RNA consortium number (https://www.broadinstitute.org/rnai/trc).
** Sources other than the TRC database or published sequences, shRNAs were designed with an online tool at http://sirna.wi.mit.edu with accession / GI numbers as inputs.

SUPPLEMENTAL EXPERIMENTAL PROCEDURES

Antibodies and reagents. The rabbit polyclonal antisera against ERα (HC-20), H2B (FL-126) and H4 (H-97), the mouse monoclonal against FOXA1 (A-3), and the goat polyclonal anti-RNF40 (S-12) were from Santa Cruz Biotechnologies; the rabbit polyclonal antisera against RNF20 (A300-715A) and INO80 (A303-371A) were from Bethyl Laboratories; the mouse monoclonal anti-GAPDH (6C5), the goat polyclonal anti-FOXA1 (ab5089), the rabbit polyclonal antisera against H2A.Z (ab4174) and INO80 (ab118787) were from Abcam; the mouse monoclonal anti-H2Bub1 (MM-0029) was from Medimabs; the mouse monoclonals against α-tubulin (T9026) and Flag (antibody M2, F3165) were from Sigma. The proteasomal inhibitor MG132 (Enzo Life Sciences) was used at 10 μM.

Cell Culture. Human embryonic kidney (HEK293T), human breast carcinoma (MDA-MB134 (Cailleau et al., 1974); a gift from Wilbert Zwart) and human lung carcinoma (A549) cells were maintained in Dulbecco's Modified Eagle's Medium (DMEM) supplemented with 10% fetal bovine serum and 1% penicillin/streptomycin. For transfection and induction experiments, cells were cultured for at least 72 hours before induction in DMEM without phenol red supplemented with 5% charcoal-stripped fetal bovine serum, 2 mM L-Glutamine and 1% penicillin/streptomycin ("white medium").

Plasmids. The following plasmids were used: the empty plasmids p3xFlag/MCS and pcDNA3.1(+) (Invitrogen). The luciferase reporters EREtkLuc (also called XETL) (Bunone et al., 1996) for ERα, GREtkLuc (also called XG46TL) for GR, the pGL2-based construct PRE-TATA-Luc (a gift from D. McDonnell) for PR, the luciferase reporter corresponding to XETL and XG46TL without enhancer (also called XTL), GK1 (Webb et al., 1998) for Gal4 fusions and the Renilla luciferase transfection control pRL-CMV (Promega); HEG0 for wild-type ERα (Tora et al., 1989), pSG5-hPR (Scheidegger et al., 2000) for PR, the vector series pSCTEV gal93 for expression of Gal4 DNA binding domain (DBD, aa 1-93) fusions (Seipel et al., 1992) and the derivatives Gal93.ER(G) containing the ERα hormone binding domain and AF2 (aa 282-595) (Maggiolini et al., 2001) or the N-terminal AF1 (aa 82-152) (Gburcik et al., 2005); expression vectors for the Flag-tagged human histone H2B and the corresponding double mutant K120R/K125R (Minsky et al., 2008). The expression vector pCMV-hGR for GR was obtained by inserting the coding region for human GR into vector pCMV5, and those for 3xFlag-RNF20 and 3xFlag-RNF40 or untagged RNF20 and RNF40 by inserting the human RNF20 and RNF40 ORFs into plasmid p3xFlag/MCS, a derivative of plasmid p3xFlag-CMV-10 (Sigma), or into plasmid pHAGE-CMV-fullEF1a-IRES-ZsGreen (plasmid ID 233 from the DNA Resource Core at the Harvard Medical School, Boston), respectively. The shRNA constructs were generated with vector pLKO.1 (Open Biosystems) according to the details given in Table S2. Lentiviruses were generated with plasmids pMD2G and psPAX2 (a gift from Didier Trono's laboratory).

Lentivirus-mediated knockdowns. HEK293T cells were seeded to a density of 1.5 millions per 100 mm-dish in standard medium 24 hours before PEI transfection with plasmids pMD2G, psPAX2 and the shRNA-encoding pLKO plasmids. 16 hours later, the medium was changed to white medium and lentivirus-containing supernatants were collected every 8-12 hours during 36 hours. Cells were infected by the lentivirus-containing supernatants during 72 hours. After infection, cells were collected for experiments. To avoid phenotype variations upon long-term shRNA-mediated knockdowns, newly infected sets of cells were used each time.

Luciferase assays. Cells were seeded in white medium and transfected with PEI with an expression vector for ERα, GR or PR (only for HEK293T), a luciferase reporter plasmid and pRL-CMV. After 18 hours, the medium was changed to fresh white medium and cells were treated for 24 hours. Cells were then lysed using the Passive Lysis Buffer (Promega) and firefly luciferase and Renilla activities were measured in cell lysates with the Dual-Luciferase kit (Promega) with a bioluminescence plate reader. Renilla activity was used as a transfection control.

Protein extraction and coimmunoprecipitation. Cells were washed once and harvested with phosphate-buffered saline (PBS), pelleted and lysed with ice-cold lysis buffer (10 mM Tris-HCl pH 7.5, 50 mM NaCl, 1 mM EDTA, 1 mM DTT, 10% glycerol, 10 mM Na-molybdate and protease inhibitor cocktail (Roche)). Cell lysates were sonicated during 15 cycles of 15 seconds at high power using a Bioruptor sonicator (Diagenode). Cell debris were discarded by centrifugation and protein concentrations were measured with the Bradford assay. For immunoprecipitation, 2 mg of proteins were incubated overnight at 4°C on a rotating wheel with a specific antibody or a control antibody of the same species (control IgG). 20 μl of protein G-dynabeads (Life Technologies), equilibrated with the lysis buffer, were then added and incubated for 3 hours at 4°C. Dynabeads were harvested with a magnetic stand and washed 3 times with 0.1% Triton X-100 in lysis buffer followed by a wash with the lysis buffer only. Proteins were eluted with a reducing buffer (sample buffer with 10 mM DTT) in boiling water for 5 minutes and beads were removed from the protein elutions with a magnetic stand.

Immunoblots. Protein extracts were mixed with the reducing buffer and heated in boiling water for 5 minutes. Protein extracts and protein elutions from immunoprecipitations were separated by SDS-PAGE and transferred to a nitrocellulose membrane. Membranes were then saturated with 5% milk in Tris-buffered saline with 0.2% Tween-20 (TBS-T) for 30 minutes and incubated overnight at 4°C with a primary antibody. Membranes were washed thrice with TBS-T and incubated for 2 hours at room temperature with a secondary antibody coupled to Horse Radish Peroxidase (HRP) (Dako). After five washes of the membranes with TBS-T, protein bands were visualized with ECL (Enhanced ChemiLuminescence, Advansta).

RNA extraction. Cells seeded in 6-well plates were lysed with guanidium-acid-phenol as described (Chomczynski and Sacchi, 1987). 2 M Na-acetate pH 4, aquaphenol and chloroform:isoamyl alcohol (49:1) were added to the lysates and vigorously mixed by vortexing. Organic and aqueous phases were separated by centrifugation at 10,000 rpm for 5 minutes and the top phases were collected. RNA was precipitated by the addition of absolute isopropanol and a centrifugation at 16,000 g for 20 minutes at 4°C. RNA pellets were washed with 80% ethanol and centrifuged at 13,000 rpm for 5 minutes at 4°C. The pellets were dried at room temperature and resuspended in nuclease-free water. RNA concentrations, and the 260/280 and 260/230 ratios were measured with a Nanodrop.

Reverse-transcription and quantitative PCR. RNA extracts were digested with RNase-free DNase (Promega) according to the manufacturer's instructions. 400 ng RNA were reverse-transcribed to cDNA with random primers (Promega), GoScript buffer (Promega) and reverse-transcriptase (Promega) according to the manufacturer's instructions. For the quantification of antisense RNA, specific primers instead of random primers were used for the reverse-transcription: 5'- TTCAGACCCCCATGCACTAC-3' for *GREB1* antisense transcripts, and 5'- AATATTTACTGAGCACCATTTGTGT-3' for *TFF1* antisense transcripts. cDNAs were mixed with the GoTaq master mix (Promega) and with specific primer pairs (Table S1) for real-time qPCR with a Biorad CFX96 thermocycler according to the manufacturer's instructions. RNA levels were standardized with *GAPDH* as the internal standard.

Chromatin immunoprecipitation (ChIP). Cells plated in 15 cm-dishes were cross-linked with 1% formaldehyde in medium for 10 minutes under gentle rotation. The cross-linking reaction was stopped by the addition of 125 mM L-glycine and the cells were washed thrice with ice-cold PBS. They were harvested in lysis buffer 1 (50 mM Hepes-KOH pH 7.5, 140 mM NaCl, 1 mM EDTA, 10% glycerol, 0.5% of NP-40 and 0.25% Triton X-100), incubated on a rotating wheel for 10 minutes at 4°C and nuclei were pelleted at 2,000 g for 5 minutes.

For ChIP assays using sonication to shear the DNA, pellets of nuclei were resuspended in lysis buffer 2 (10 mM Tris-HCl pH 8.0, 200 mM NaCl, 1 mM EDTA and 0.5 mM EGTA), incubated on a rotating wheel for 5 minutes and pelleted at 2,000 g for 5 minutes. Pellets were lysed with lysis buffer 3 (10 mM Tris-HCl pH 8.0, 100 mM NaCl, 1 mM EDTA, 0.5 mM EGTA, 0.1% Na-deoxycholate, 0.5% N-lauroylsarcosine and a protease inhibitor cocktail (Roche)) and chromatin was sheared by 30 cycles of 30 seconds of sonication at high power with a bioruptor sonicator. 0.1% Triton X-100 was added, cell membranes were discarded by centrifugation at 16,000 g for 10 minutes and nuclear extracts were collected.

For ChIP assays using MNase digestion of the chromatin, we adapted a published protocol (Infante et al., 2012). After the step with the lysis buffer 1, pellets of nuclei were resuspended in the NPS buffer (0.5 mM spermidine, 0.075% NP-40, 50 mM NaCl, 10 mM Tris-HCl pH 7.5, 5 mM $MgCl_2$ and 1 mM $CaCl_2$) and centrifuged for 5 minutes at 2'000 g. Pellets were resuspended with 1 ml of NPS buffer, 1 u of MNase was added and incubated at 37°C for 30 minutes. These conditions were optimal for our experiments to get primarily mononucleosomes. The reaction was stopped by the addition of 15 mM EDTA and 3 mM EGTA. The buffer L (final working concentrations: 50 mM Hepes-KOH, pH 8.0, 140 mM NaCl, 1 mM EDTA, 1% Triton X-100 and 0.1% sodium deoxycholate) along with protease inhibitors was added to the samples, and they were gently sonicated with 4 cycles of 20 seconds at low power. Samples were centrifuged 10 minutes at 16'000 g and nuclear extracts were collected.

From here on, the protocol is the same for both ChIP methods. 10 µl of nuclear extracts were saved to measure the inputs and the rest was incubated overnight at 4°C on a rotating wheel with dynabeads that were pre-coated during 3 hours with a specific antibody in PBS containing 0.5% BSA. Dynabeads were harvested with a magnetic stand and washed 10 times with RIPA buffer (50 mM Hepes-KOH pH 7.5, 500 mM LiCl, 1 mM EDTA, 1% of NP-40, 0.7% Na-deoxycolate). A last wash with TBS was done and reverse-crosslinking of the inputs and of the dynabeads were performed with the elution buffer (50 mM Tris-HCl pH 8, 10 mM EDTA and 1% SDS) at 65°C overnight under agitation at 900 rpm. Eluates were separated from the dynabeads with a magnetic stand and collected in new tubes. Samples were diluted in TE buffer and incubated with 25 µg/ml RNase for 1 hour at 37°C followed by an incubation with 200 µg/ml proteinase K for 2 hours at 55°C. DNA was

isolated with phenol:chloroform:isoamyl alcohol (25:24:1), transferred to Phase Lock Gel Light tubes (5 PRIME) and centrifuged at 10,000 rpm for 5 minutes. Top phases were collected in new tubes containing 10 µg glycogen in 200 mM NaCl. Absolute ethanol was added, samples were mixed, incubated 20 minutes at -80°C and centrifuged at 16,000 g for 30 minutes at 4°C. Pellets were washed with 80% ethanol, centrifuged at 16,000 g for 5 minutes and dried 30 minutes at room temperature. Pellets were resuspended in nuclease-free water. Quantitative PCR was performed with the primers of Table S1. ChIP values were standardized with internal controls (the *c-MYC* intron for the ChIP of ERα and FOXA1, or the *GAPDH* coding region for the ChIP of H2A.Z, H4, H2B, H2Bub1 and INO80) and normalized with the input values.

SUPPLEMENTAL REFERENCES

Bunone, G., Briand, P.A., Miksicek, R.J., and Picard, D. (1996). Activation of the unliganded estrogen receptor by EGF involves the MAP kinase pathway and direct phosphorylation. EMBO J. *15*, 2174-2183.

Cailleau, R., Young, R., Olive, M., and Reeves, W.J., Jr. (1974). Breast tumor cell lines from pleural effusions. J. Natl. Cancer Inst. *53*, 661-674.

Chomczynski, P., and Sacchi, N. (1987). Single-step method of RNA isolation by acid guanidinium thiocyanate-phenol-chloroform extraction. Anal. Biochem. *162*, 156-159.

Gburcik, V., Bot, N., Maggiolini, M., and Picard, D. (2005). SPBP is a phosphoserine-specific repressor of estrogen receptor α. Mol. Cell. Biol. *25*, 3421-3430.

Infante, J.J., Law, G.L., and Young, E.T. (2012). Analysis of nucleosome positioning using a nucleosome-scanning assay. Methods Mol. Biol. *833*, 63-87.

Maggiolini, M., Bonofiglio, D., Marsico, S., Panno, M.L., Cenni, B., Picard, D., and Ando, S. (2001). Estrogen receptor α mediates the proliferative but not the cytotoxic dose-dependent effects of two major phytoestrogens on human breast cancer cells. Mol. Pharmacol. *60*, 595-602.

Minsky, N., Shema, E., Field, Y., Schuster, M., Segal, E., and Oren, M. (2008). Monoubiquitinated H2B is associated with the transcribed region of highly expressed genes in human cells. Nat. Cell Biol. *10*, 483-488.

Rosenbluh, J., Nijhawan, D., Cox, A.G., Li, X., Neal, J.T., Schafer, E.J., Zack, T.I., Wang, X., Tsherniak, A., Schinzel, A.C. et al. (2012). β-catenin-driven cancers require a YAP1 transcriptional complex for survival and tumorigenesis. Cell *151*, 1457-1473.

Sarbassov, D.D., Guertin, D.A., Ali, S.M., and Sabatini, D.M. (2005). Phosphorylation and regulation of Akt/PKB by the rictor-mTOR complex. Science *307*, 1098-1101.

Scheidegger, K.J., Cenni, B., Picard, D., and Delafontaine, P. (2000). Estradiol decreases IGF-1 and IGF-1 receptor expression in rat aortic smooth muscle cells. Mechanisms for its atheroprotective effects. J. Biol. Chem. *275*, 38921-38928.

Seipel, K., Georgiev, O., and Schaffner, W. (1992). Different activation domains stimulate transcription from remote ('enhancer') and proximal ('promoter') positions. EMBO J. *11*, 4961-4968.

Tora, L., Mullick, A., Metzger, D., Ponglikitmongkol, M., Park, I., and Chambon, P. (1989). The cloned human oestrogen receptor contains a mutation which alters its hormone binding properties. EMBO J. *8*, 1981-1986.

Webb, P., Nguyen, P., Shinsako, J., Anderson, C., Feng, W., Nguyen, M.P., Chen, D., Huang, S.M., Subramanian, S., McKinerney, E. et al. (1998). Estrogen receptor activation function 1 works by binding p160 coactivator proteins. Mol. Endocrinol. *12*, 1605-1618.